이 학 석 사 학 위 논 문

프로테오로돕신을 함유하는 SAR116-clade 균주 *Candidatus* Puniceispirillum marinum IMCC1322의 분리, 배양 및 유전체 분석

2019년 2월

부경대학교 과학기술융합전문대학원

해양바이오융합과학전공

이 준 학

이 학 석 사 학 위 논 문

프로테오로돕신을 함유하는 SAR116-clade 균주 *Candidatus* Puniceispirillum marinum IMCC1322의 분리, 배양 및 유전체 분석

지도교수 오 현 명

이 논문을 이학석사 학위논문으로 제출함.

2019년 2월

부경대학교 과학기술융합전문대학원

해양바이오융합과학전공

이 준 학

이준학의 이학석사 학위논문을 인준함

2019년 2월

위 원 장 이학박사 조 영 근 (인)

위 원 이학박사 이 준 희 (인)

위 원 이학박사 오 현 명 (인)

목 차

List of Tables and Figures

Isolation, Cultivation, and Genome Analysis of Proteorhodopsin-Containing SAR116-clade strain *Candidatus* Puniceispirillum marinum IMCC1322

Jun Hak Lee

Specialized Graduate School Science & Technology Convergence

Pukyong National University

Abstract

Strain IMCC1322 was isolated from a surface water sample from the East Sea of Korea. Based on 16S rRNA analysis, it was found to belong to the OCS28 sub-clade of SAR116. The cells appeared as short vibrioids in logarithmic-phase culture, and elongated spirals during incubation with mitomycin or in aged culture. Growth characteristics of strain IMCC1322 were further evaluated based on genomic information. The IMCC1322 genome encodes proteorhodopsin (PR), carbon monoxide dehydrogenase, and dimethylsulfoniopropionate (DMSP)-utilizing enzymes. IMCC1322 PR was characterized as a functional retinylidene protein that acts as a light-driven

proton pump in the cytoplasmic membrane. However, the PR-dependent phototrophic potential of strain IMCC1322 was only observed under CO-inhibited and nutrient-limited culture conditions. A DMSP-enhanced growth response was observed in addition to cultures using sodium formate and methane sulfonate. Strain IMCC1322 cultivation analysis revealed biogeochemical processes characteristic of the SAR116 group, a dominant member of the microbial community in euphotic regions of the ocean. The polyphasic taxonomy of strain IMCC1322 is proposed as *Candidatus* Puniceispirillum marinum, and was confirmed by chemotaxonomic tests, in addition to 16S rRNA phylogeny and cultivation analyses.

Ⅰ. Introduction

Alphaproteobacteria [e.g., SAR11, *Roseobacter*-clade affiliated (RCA) bacterial cluster, and SAR116] and Gammaproteobacteria (e.g., SAR86) constitute the most abundant heterotrophic taxa in the open ocean (Giovannoni SJ and Rappé MS, 2000). Clade SAR116 was previously described in a microbial community study of the oligotrophic Sargasso Sea (Britschgi TB and Giovannoni SJ, 1991; Giovannoni SJ *et al.*, 1990). This unique Alphaproteobacteria taxon has also been isolated from the North Carolina Ocean Margin, Aloha in the North Pacific Gyre, and from the Oregon Coast plankton samples (Mullins TD *et al.*, 1995; Rappé MS *et al.*, 1997). SAR116 has been identified as a ubiquitous uncultured lineage of marine bacterioplankton (Giovannoni SJ and Rappé MS, 2000) (see Supporting Information and Table 3). Further, 16S rDNA clones of SAR116 have been retrieved from such sites as estuaries, coastal regions, marginal seas, pelagic oceans, Polar Regions, and deep-sea environments. It is also found in the vicinity of salt marsh creeks, marine sponges, and coral reef samples (see Supporting Information and

Table 4).

SAR116 accounts for approximately 5% of the marine bacterial clone libraries (Giovannoni SJ and Rappé MS, 2000; Rappé MS *et al.*, 1997). The relative abundance of clones of the dominant bacterial species in open oceans, ocean margins, and coastal regions has been previously categorized as SAR11 > RCA > SAR86 > SAR116 (Giovannoni SJ and Rappé MS, 2000). Based on preliminary analysis (Table 4), SAR11 accounts for 17.0% (range: 0–47.2%) of marine bacterial communities; RCA cluster bacterial clones, identified less frequently, account for 8.7% of marine bacterial communities (range: 0–38.63%); and SAR116 and SAR86 represent 7.0% (range: 0.6–22.2%) and 4.0% (range: 0–26.5%), respectively, of the bacterial 16S rDNA clone libraries analyzed (Table 4).

Proteorhodopsin (PR), isolated from bacteria from the SAR86 group, has sparked interest in light-driven processes in recent decades (Bano N and Hollibaugh JT, 2002a; Beja O *et al.*, 2001; Gomez-Consarnau L *et al.*, 2007). SAR86 bacteria remain the only uncultured and unexplored group, although SAR86 genomes have been sequenced using single-cell genomic approaches (Dupont CL *et al.*, 2012). Genomes of SAR11 and SAR116 were also found to encode PR (Giovannoni SJ *et al.*,

2005; Oh HM *et al.*, 2011; Oh HM *et al.*, 2010), and the phototrophic abilities of PR-bearing marine bacteria have been studied in *Flavobacteria* (Gomez-Consarnau L *et al.*, 2007; Gonzalez JM *et al.*, 2008) and *Vibrio* species (Gomez-Consarnau L *et al.*, 2010).

The phototrophic potential of SAR116 was originally described in a microcosmic experiment of marine microbial communities using automated ribosomal intergenic spacer analysis (ARISA) (Schwalbach MS *et al.*, 2005). Strain IMCC1322 was isolated from the surface seawater of the East Sea Basin of Korea, and its genomic DNA was sequenced by whole-genome sequencing (Oh HM *et al.*, 2010). This SAR116 clade strain encodes PR, indicating its light-harvesting ability, as well as other functional genes, such as *dmdA* [dimethylsulfoniopropionate (DMSP) demethylases] and two aerobic types of carbon monoxide dehydrogenases (CODH) (Oh HM *et al.*, 2010). Later, strain HTCC8037 was cultivated from the Sargasso Sea, and was identified as a member of the SAR116 clade (Stingl U *et al.*, 2007b). However, neither functional nor genotypic studies of the photoheterotrophic genes of HTCC8037 were performed. Based on 16S rDNA similarity (98.0%), strain HIM100 is the closest relative to strain HTCC8037 (Stingl U *et al.*, 2007b). Its genome has been sequenced; the draft genome harbors functional genes also

found in strain IMCC1322 (Grote J *et al.*, 2011).

Here, we report a cultivation study of the IMCC1322 strain. The study involved genomic and metabolomic approaches, including PR characterization; evaluation of the light-dependent response and response to carbon monoxide concentration in cultures; analysis of DMSP and of other utilizable organic substrates; and polyphasic taxonomy tests.

Ⅱ. MATERIALS AND METHODS

1. *IMCC1322 Isolation and Genome Analysis*

A surface seawater sample was collected at a specific site on the East Sea of Korea (N 38° 20’ 15”, E 128° 33’ 32”), and bacterial colonies were isolated on mPYC medium (a modified R2A medium), as described previously (Reasoner DJ and Geldreich EE, 1985). The mPYC medium was prepared in autoclaved aged seawater using the following three ingredients (all from BD Difco, USA, and at a concentration of 0.5 g/l): proteose peptone no. 3 (#211693), yeast extract (#212750), and casamino acids (#223050) (Kang I *et al.*, 2013).

Diluted mPYC (0.01× mPYC), prepared in seawater agar, was used for the isolation of micro-colonies (diameter <0.05 mm). The colonies were then sub-cultured and analyzed by 16S rDNA PCR, followed by *Hae*III and/or *Hha*I restriction enzyme digestion. Subsequently, 16S rDNA from selected colonies was analyzed by Sanger sequencing, as described previously (Vergin KL *et al.*, 2001). Once the identity of strain IMCC1322 was phylogenetically confirmed, the colonies were routinely sub-cultured at 20 °C on mPYC plates, which allowed for the growth of colonies up to

0.1 mm in diameter.

Colony-derived genomic DNA was analyzed by whole-genome sequencing. Genomic DNA was prepared from IMCC1322 colonies grown on mPYC agar plates. Shotgun sequencing and the assembly of chromosomal DNA were performed by Macrogen, Inc. (Seoul, Korea). ORF prediction and annotation were performed by using EMFAS software (Ensoltek, Daejeon, South Korea) based on homology searches of the NCBI/UniProt databases and non-homology-based functional annotations (Oh HM *et al.*, 2010).

2. *Phylogenetic Analysis*

For the construction of 16S phylogenetic trees and sequence alignment, ARB package (Ludwig W *et al.*, 2004) and Release 106 of the SSU database of SILVA (http://www.arb-silva.de) (Pruesse E *et al.*, 2007) were used. The determination of sequence similarity and taxon selection

were performed using ARB; the phylogenetic trees were generated using PAUP 4.0 beta 10 (Swofford D, 2002), as described previously (Cho JC and Giovannoni SJ, 2006). Nucleotide alignments were exported from ARB and two tree-building methods were used: neighbor-joining (NJ) and maximum parsimony (MP). Bootstrap values of 1000, and 1000 replicates were used for NJ and MP, respectively.

For phylogenetic analysis of PR, PF01036 alignments were downloaded from pfam 23.0 (Finn RD *et al.*, 2008). The NJ and MP methods were used for amino acid alignments of bacteriorhodopsin (PF01036; http://pfam.sanger.ac.kr). Selected subsets of NCBI alignments for phylogenetic analyses were done using PAUP 4.0 beta 10 (Swofford D, 2002) with bootstrap values of 1000 (NJ) and 100 (MP) replicates.

3. *Transmission Electrom Microscopy (TEM)*

Actively growing cells were treated overnight with 0.5 μg/ml mitomycin C (#M4287, Sigma Aldrich, St. Louis, MO, USA). The cells were fixed overnight in 2.5% glutaraldehyde (G0449, Samchun Chemical, Korea) at 4 °C. Fixed cells were transferred onto 200-mesh copper grids

(#CF2W-Cu, EMS, USA) by ultracentrifugation at 120,000 × *g* for 30 min. The grids were then negatively stained with uranyl acetate (Noble RT and Fuhrman JA, 1998) for TEM analysis (CM200; Philips, Netherlands).

4. *Direct Cell Counting and Growth Curve Analysis*

For direct cell counts, initial inoculums of 1.0×10^4 cells/ml were cultured in 30 ml of medium in acid-washed polycarbonate oak-ridge tubes (#3118-0050, Nalgene, Rochester, NY, USA). Triplicate cultures at 4 °C, 10 °C, 15 °C, and 20 °C were sampled by withdrawing 180-μl aliquots, formalin-fixed and counted after 4′,6-diamidino-2-phenylindole (DAPI) staining (#D9542, Sigma Aldrich) (Connon SA and Giovannoni SJ, 2002). Ten counts per sample were averaged to plot the growth curves. Direct cell counting was performed using an epifluorescence microscope equipped with a digital camera (Nikon 80i, Nikon, Japan), as described previously (Connon SA and Giovannoni SJ, 2002). Briefly, the cells were fixed with formalin (final concentration 0.875%, v/v), stained with DAPI (final concentration 7.5 μg/ml), and filtered through 0.2-μm pore-sized Nuclepore track-etched membranes (23-mm diameter; #110606,

Whatman, Maidstone, UK). The filters were mounted on an objective slide and embedded in low-fluorescence type FF immersion oil (#16212, Cargille Laboratories, Cedar Grove, NJ, USA).

Growth curves were also analyzed at different temperatures, salinities, and hydrogen ion concentrations using a temperature-gradient shaking incubator (TVS 126MA, Advantec Toyo, Japan). The growth of strain IMCC1322 with different concentrations of DMSP in mPYC was also examined using a temperature-gradient shaking incubator. Unless otherwise stated, all culturing experiments were performed at 20 °C.

5. *Spectral Properties of PR from IMCC1322*

The PR spectra were acquired using standard 1-cm cuvettes and a Shimadzu UV-visible spectrophotometer (UV-2550), with IMCC1322 cells harvested from mPYC liquid cultures. The transient absorption spectra of light-exposed IMCC1322 cells were acquired using an Olis RSM optical spectroscope. The excitation flash (10-mJ pulse) at 532 nm was supplied by a (Nd:YAG) Minilite-II laser (Continuum, CA, USA). Probe

beams transmitted through the samples were passed through a notch filter (model RNF-532.0; CVI Laser). The preparation of bacterial strains and plasmids (pKJ900 and pORANGE), expression and purification of PR, and pK_a determinations were performed as described previously (Kim SY *et al.*, 2008).

6. *Effect of Light and CO Supplementation*

For light exposure-enhanced growth curves, the cells were grown in 0.1× mPYC in autoclaved and 0.22-μm cellulose acetate membrane-filtered seawater under cool-white light at an intensity of 70 μmol m^{-2} s^{-1} for 24 h per day, or in darkness. The cultures were sampled on a daily basis and the cells were counted using the DAPI-staining method described above. To test the effect of CO on cell growth, nutrient-constrained conditions were simulated by growth in 0.01× mPYC, with or without light exposure. Each 100-ml serum bottle containing 50 ml of the culture medium was inoculated with 5 × 10^6 freshly grown cells, and sterile-filtered 10 ml of CO was injected into the headspace over CO gas amended culture (approximately 50 ml air). DAPI-stained cells were

counted with or without light exposure, as described above. As a control, cultures in 0.05× mPYC were grown in constant darkness without CO.

7. *LED for Pure Green Light Illumination*

Different illumination sources were used to confirm whether the PR-bearing IMCC1322 cells could utilize light energy from a CFL (fluorescent P-type lamp, Philips). An alternative light source that corresponded to the spectroscopic properties of PR from IMCC1322 was also used. An LED device was built to order by Anyang (Korea); pure green LED dots on a strip (30 × 20) were arrayed on incubator-sized aluminum plates (57 cm × 40 cm). The wavelength of the light was 525 nm (according to the manufacturer's specification sheet).

The effect of LED and CFL was determined using a fiber optic spectrophotometer, SV2100 VIS [Korea Materials & Analysis Corp. (K-MAC), Daejeon, Korea]. VisualSpectra 2.1 SR software (K-MAC) was used for spectral data acquisition, and each spectrum was plotted to compare the distribution of wavelengths therein. Data were visualized using Mathematica 10.4 software (Wolfram Research, Champaign, IL,

USA).

8. *Determination of Biochemical Characteristics*

Biochemical characteristics of strain IMCC1322 were investigated using API arrays (API 20NE, API ZYM; BioMérieux Korea, Seoul, Korea), prepared according to the manufacturer's instructions with the following modifications: the strips were inoculated with 5×10^5 IMCC1322 cells/ml in artificial seawater (Choo YJ *et al.*, 2007) and incubated at 20 °C for 7 d. Starch hydrolysis was determined using mPYC agar containing 0.5 g/l Difco soluble starch (#217802, BD Co., Franklin Lakes, NJ, USA). Additional carbon sources were individually tested at a concentration of 100 μM in mPYC medium. The carbon sources are listed in Table 10.

9. *Antibiotic Resistance Determination*

Ten different antimicrobial agents (listed in the species description and in the Results section) were tested by using the diffusion plate method (Jorgensen JH *et al.*, 1999) on mPYC agar. The plates were

incubated for 4 weeks at 25 °C.

10. *Analysis of Cellular Fatty Acid Profiles*

FAMEs were prepared from cultures grown in mPYC medium at 20 °C for 6 d. They were analyzed by using the Sherlock Microbial Identification System ver. 6.1 (MIDI Inc., USA), “instant method” with the RTSBA6 library database from MIDI ver. 6.1.

Polar lipids were extracted from freeze-dried cultures of strain IMCC1322 according to a previously described method (Minnikin DE *et al.*, 1984). Polar lipids extracted by chloroform/methanol were separated by two-dimensional thin-layer chromatography using silica gel 60 F254 aluminum-backed thin-layer plates (Merck, Darmstadt, Germany). The solvent system for the first dimension was chloroform/methanol/water (65:24:4, v/v), and that for the second dimension was chloroform/glacial acetic acid/methanol/water (40:7.5:6:1.8, v/v). The separated components were visualized by treating plates with 10% (w/v) molybdatophosphoric acid, followed by heating at 150 °C for 10 min. Glycolipids were detected by spraying the plate with 0.5% (w/v) α-naphthol in methanol/water (1:1)

and then with sulfuric acid/ethanol (1:1), followed by heating at 100 °C for 5 min; phospholipids were finally detected using the Zinzadze reagent (Minnikin DE *et al.*, 1984).

Ⅲ. Results

1. *Isolation and 16S rDNA Phylogeny of Strain IMCC1322*

The strain IMCC1322 was isolated from an unexpected colony formed on a traditional agar plate. The phylogenetic relationship of IMCC1322 with its uncultured and closely related 16S rDNA clones is depicted in Fig. 1. The obtained 16S rRNA sequences were aligned with 66 nucleotide sequences from cultured Alphaproteobacteria strains and uncultured clones, including ones from the SAR116 clade. The Kimura 2-parameter model was used for genetic distance analysis that entailed 1167 nucleotides (298 bases were excluded from the 1465-base set of 16S rRNA sequences) (Fig. 1). The SAR116 cluster is comprised of several well-defined sub-groups, including the SAR11 clade (Rappé MS *et al.*, 1997). The 16S rRNA molecular sequences closest to SAR11 were obtained from uncultured clones and metagenomic studies (Fig. 1).

According to previous marine bacterioplanktonic community studies (Britschgi TB and Giovannoni SJ, 1991; Giovannoni SJ and Rappé MS, 2000; Mullins TD *et al.*, 1995; Rappé MS *et al.*, 1997; Treusch

AH *et al.*, 2009), SAR116 includes the subgroups OCS28, OM25/OCS24, OCS126/OM38, and HOC (Fig. 1). The 16S rDNA sequence analysis revealed the following similarities of strain IMCC1322 to the representative clones analyzed: 97.8% identity with OCS28 (GenBank acc. no. AF001636); 94.2% identity with uncultured Proteobacteria OM25/OCS24 (U70678/AF001637); 92.5% identity with uncultured Alphaproteobacteria HOC26/HOC7 (AB054160/AB054141); and 91.8% identity with uncultured Proteobacterium OCS126 (AF001638). We therefore concluded that strain IMCC1322 belongs to the OCS28 subgroup of SAR116, a previously reported environmental 16S rDNA clone from the Oregon Coast and continental shelf off North Carolina (Rappé MS *et al.*, 1997).

2. *Cell Shape and Colony-Forming Ability of Strain IMCC1322*

Initially, IMCC1322 cells displayed vibrioid morphology (Fig. 2A), but actively growing cells underwent morphological change to spiral forms upon overnight treatment with mitomycin C (0.5 μg/ml) (Fig. 2B), or after

prolonged incubation past the late-logarithmic phase (data not shown). The genome of strain IMCC1322 harbors a medium-sized prophage sequence (Oh HM *et al.*, 2010). Therefore, lysogenic induction with the lysogenic induction agent mitomycin C was attempted and cells were analyzed by transmission electron microscopy (TEM) (Rachel TN and Jed AF, 1998). However, only change from elongated vibrioids to spiral forms was observed (Fig. 2B), with no phage particles apparent. When single-cells of strain IMCC1322 were grown in culture (Fig. 2A), morphological changes were also observed in cultures past the late-logarithmic phase (Fig. 2B). The cells reverted to the single vibrioid form upon transfer to fresh medium. The average cell size of exponentially-growing IMCC1322 cells (Fig. 2A) was 2.72-μm long (σ = ± 0.581 μm, n = 30) and 0.377-μm wide (σ = ± 0.0416 μm, n = 30); in the stationary phase, the average cell size was 2.01-μm long (σ = ± 0.546 μm, n = 30) and 0.375-μm wide (σ = ± 0.0420 μm, n = 30). The mitomycin-C-induced spiral forms of IMCC1322 cells (Fig. 2B) were 6.03-μm long (σ = ± 0.540 μm, n = 30) and 0.319-μm wide (σ = ± 0.0510 μm, n = 30).

Basic colony evaluation and growth characteristics, including temperature, pH, and salinity ranges, are summarized in Table 5. Pale

reddish colonies of strain IMCC1322 were observed on a mPYC agar plates, with a diameter of 0.05–0.1 mm. The colonies were circular, smooth, entire, opaque, and convex. Gliding motility was not apparent. The pale reddish colony color may have been associated with the PR gene and a series of retinoid genes downstream of PR (Oh HM *et al.*, 2010), as explained below.

3. *Optimal Temperature, pH, and Salinity for the Growth of Strain IMCC1322*

The optimum temperature, pH, and salinity values for strain IMCC1322 were investigated using the temperature-gradient incubator TVS-126MA (Table 3): the temperature range for growth was determined to be 12.8–34.2 °C, with the optimum growth temperature at 25.5 °C, and the expected doubling time of 18 h (Fig. 7). The optimal pH for IMCC1322 cultivation was determined to be 7.0 (Fig. 8). The cells were grown in modified R2A (mPYC) medium prepared in 60%, 80%, and 100% seawater, or seawater supplemented with 0.25 M NaCl. Seawater contains 0.45 M [Na^+], or approximately 2.6% NaCl (Macleod RA, 1965);

therefore, IMCC1322 cell growth required 1.6–4.0% (w/w) NaCl in mPYC (Fig. 9). Optimal growth of strain IMCC1322 was observed in mPYC medium supplemented with ca. 2.1–2.6% NaCl (w/w). This corresponded to mPYC with a salt level of 80–100% of that of seawater (Fig. 9). The optimal DMSP concentrations were also tested in the mPYC medium.

4. *Antibiotic Resistance and Cellular Fatty Acid Content*

The strain IMCC1322 was resistant to gentamycin (10 μg/ml), but was sensitive to ampicillin (10 μg/ml), chloramphenicol (25 μg/ml), erythromycin (15 μg/ml), kanamycin (30 μg/ml), penicillin G (10 μg/ml), rifampicin (50 μg/ml), streptomycin (10 μg/ml), tetracycline (30 μg/ml), and vancomycin (30 μg/ml).

Phosphoethanolamine and an unknown phosphoglycolipid were detected in IMCC1322 cultures (Fig. 10). The fatty acid methyl ester (FAME) profiles revealed the presence of polyunsaturated fatty acids (PUFAs)(Table 6). Cellular fatty acids of strain IMCC1322 had carbon chain lengths of C_{10}–C_{20}; FAMEs included saturated, unsaturated,

cyclohydroxylated, and hydroxylated components (Table 6). The dominant cellular fatty acids were Summed Feature 3 ($C_{16:1}\omega7c/C_{16:1}\omega6c$, 49.78%), Summed Feature 8 ($C_{18:1}\omega7c/C_{18:1}\omega6c$ 39.98%), and $C_{16:0}$ (3.08%) (Table 6). Interestingly, strain IMCC1322 was able to produce the PUFAs eicosa-5,8,11,14-tetraenoic acid ($C_{20:4}\omega6,9,12,15c$) or arachidonic acid (AA).

5. *Genome Summary*

The completed genome of strain IMCC1322 was obtained using whole-genome shotgun sequencing (Oh HM *et al.*, 2010). The bacterium has a 2,753,527-bp circular genome (48.85% G+C content) with one rRNA operon (GenBank acc. no. CP001751) (Oh HM *et al.*, 2010). Based on the metabolic capabilities deduced from the predicted open reading frames (ORFs), strain IMCC1322 is an aerobic heterotrophic bacterium (Table 1). The IMCC1322 genome contains genes involved in the Krebs cycle, and pentose phosphate and gluconeogenesis pathways. However, the Embden-Meyerhof-Parnas pathway is incomplete, as a gene for 6-phosphofructokinase was not identified. The Entner-Doudoroff pathway is present, as confirmed by the presence of 6-phosphogluconate

dehydratase and 2-dehydro-3-deoxyphosphogluconate aldolase genes. Strain IMCC1322 also encodes a dimethyl sulfoxide (DMSO) reductase and harbors a gene for glycine/serine hydroxymethyltransferase, allowing it to use an assimilatory serine cycle for formaldehyde assimilation. The bacterium also possesses genes encoding formate dehydrogenase and methanesulfonate (MSA) monooxygenase. Autotrophic carbon fixation pathways were not identified in the IMCC1322 genome, and genes for ribulose-1,5-bisphosphate carboxylase oxygenase, reversed tricarboxylic acid cycle, reductive acetyl-CoA pathway, 3-hydroxypropionate/4-hydroxybutyrate cycles, etc., were absent (Table 1). The encoded genes included secondary metabolism genes, xenobiotic degradation genes, membrane transporter genes, and regulatory genes. Many genes for secondary metabolite production and xenobiotic degradation were annotated (Table 7). The genome also encodes such enzymes, as oxidoreductase, oxygenases, aryl-compound related enzymes, and retinoid biosynthesis genes (as described below). Further, genes for nitrate reductase, sulfate reductase, the phosphate regulon sensor PhoR, high-affinity ATP-binding cassette (ABC) phosphate transporter system, polyphosphate kinase, and exopolyphosphatase/GppA phosphatase were identified (Table 8 and Table 9). Membrane transport genes included

genes encoding ABC transporters for various substrates, unknown ABC transporters, antiporter- and symporter-related sodium ion transporters, tripartite ATP-independent periplasmic (TRAP) transporters for dicarboxylates, and others (Table 7). The metabolic regulatory genes were nitrogen/sulfur/phosphorus uptake genes and metalloregulators. The identified antibiotic resistance genes are summarized in Table 8. The SOS repair system and stress-related genes, as well as transcriptional regulators, were also annotated. Further, sigma factor-related genes including σ^{54} (fis family); RNA polymerase subunits σ^{28} (FliA/WhiG), σ^{70} (RpoD), and σ^{32}(RpoH); ρ (transcription termination factor); anti-σ^{28} factor (FlgM); and anti-anti-sigma regulatory factor (spoIIAA) were identified (Table 8).

Strain IMCC1322 is predicted to be a metabolic generalist, harboring functional genes for the utilization of sunlight, DMSP, CO, and C_1 compounds on the ocean surface (Oh HM *et al.*, 2010). The encoded functional genes include ones coding for PR (GenBank acc. no. ADE40369), CODH, and DMSP demethylase (*dmdA*) (Table 1), as well as other putative DMSP-lyase proteins (Table 2). Accordingly, IMCC1322 colonies were incubated with varying concentrations of DMSP as the

growth substrate. The maximal growth was observed after incubation with 50 μM DMSP (Fig. 11).

Other functional genes of biogeochemical importance harbored by strain IMCC1322 and present in the genome of strain HIMB100 (Grote J *et al.*, 2011) included genes encoding CODH, DMSP enzymes, DMSO reductase, glycine/serine hydroxymethyltransferase, and PR, as well as genes involved in retinoid biosynthesis. MSA monooxygenase was only present in the IMCC1322 genome, which is 295 kbp longer and contains 200 more genes than the draft genome contigs of strain HIMB100 (Grote J *et al.*, 2011).

6. *Phylogeny and Spectroscopic Characterization of PR from Strain IMCC1322*

Phylogenetic analysis of PR from strain IMCC1322 (Fig. 3) revealed that the protein belongs to a clade that is clearly distinct from that of rhodopsins of halophilic archaea, and of xanthorhodopsins from *Salinibacter ruber* and *Gloebacter violaceus* (Balashov SP and Lanyi JK, 2007; Beja O *et al.*, 2001), and the other previously described PRs from

the SAR11, SAR92, and SAR86 groups (Fig. 3). IMCC1322 PR belonged to a group composed of cultured HTCC2255 and some uncultured Alphaproteobacteria; its closest sister clades are SAR92, SAR86, and SAR92 (Fig. 3). The IMCC1322 PR-encoding gene is composed of 786 nucleotides and is translated into a protein of 261 amino acids. The most essential residues for a rhodopsin pump, such as the proton acceptor and proton donor sites, were conserved in the IMCC1322 PR protein. IMCC1322 PR shared 80%, 77%, and 73% identity with the predicted PRs from uncultured bacterial clones MEDPR46A6 (AAY68055), MEDPR66A3 (AAY68065), and MedeBAC82F10 (AAY78592), respectively, from the Mediterranean Sea (Sabehi G *et al.*, 2005).

In a preliminary investigation, we analyzed the carotenoid/retinal peaks of PR; no carotenoid signal was apparent (data not shown). The PR signal was indeed observed (Fig. 4) and, hence, retinal might be fully processed by the *blh* gene product (β-carotene 15,15′-dioxygenase; GenBank acc. no. SAR116_2131) in strain IMCC1322.

Biophysical methods, such as spectroscopy, light-induced difference spectroscopy, and flash-photolysis, were then used to demonstrate that the IMCC1322 PR is an authentic retinylidene protein

acting as a light-driven proton pump. Consistently with predictions based on the pink colony color (Table 5), the absorption spectra of IMCC1322 cells grown in constant darkness or with constant light exposure both exhibited a 522-nm peak (Fig. 4A).

In general, microbial rhodopsins exist as two spectral forms in a proton-dependent equilibrium: a blue-shifted alkaline species or a red-shifted acidic species. The absorption maxima of the two species of IMCC1322 PR differed by 30 nm (Fig. 4B). Flash-induced short-timescale traces, which are characteristic of pumping rather than sensory rhodopsins, were observed in suspensions of IMCC1322 cell membranes (Fig. 4C). Photochemical reactions on the IMCC1322 membranes revealed a red-shifted O intermediate (580 nm) with a decay time of 15 ms (Fig. 4D). These spectroscopic data provided direct physical evidence for the existence of PR-like transporters and endogenous retinal molecules in the microbial fraction of coastal surface waters.

Further, IMCC1322 PR displayed an acid-induced red shift (559 nm). The red shift is generally attributed to the neutralization of the Schiff base counter-ion. The IMCC1322 PR was purified and spectroscopic titration of the Schiff base counter-ion performed. The pK_a of the proton acceptor of

IMCC1322 PR was approximately 5.7 (Fig. 4C), which was lower than that of a previously reported Monterey bay PR (pK_a of approximately 7.2) (Wang WW *et al.*, 2003). When the physiological pH is higher than the pK_a, and the proton acceptor is deprotonated, PR might abstract a proton from the Schiff base during a photochemical reaction and continue its photocycle. The pH of the oceanic water where strain IMCC1322 resides is approximately 8, i.e., higher than the pK_a of IMCC1322 PR. This indicated that IMCC1322 PR could be functionally adapted to the bacterium's natural habitat. Furthermore, the absorption maximum of IMCC1322 PR produced in *Escherichia coli* matched that of the native PR from strain IMCC1322 (Fig. 4B).

7. *Cellular Growth Response to Light and Darkness*

Light-enhanced growth of strain IMCC1322 was evaluated using three different nutrient dilutions in aged seawater, as follows: 100-times diluted mPYC, 10-times diluted mPYC, and undiluted (1×) mPYC (Fig. 5A). Identification of PR and downstream retinoid biosynthesis genes on the IMCC1322 genome implied that their products could contribute to light-

stimulated growth, as in the case with *Dokdonia donghaensis* MED134 (Gomez-Consarnau L *et al.*, 2007) and *Polaribacter* sp. MED152 (Gonzalez JM *et al.*, 2008). Consequently, strain IMCC1322 was cultured in the light and darkness. PR is a light-driven proton pump (Beja O *et al.*, 2000; Beja O *et al.*, 2001; Giovannoni SJ *et al.*, 2005; Gomez-Consarnau L *et al.*, 2007), and it may help IMCC1322 outcompete other microbes at the ocean surface, acting together with the abundant ATP-independent electrochemical transporters and ABC-type transporter genes (Oh HM *et al.*, 2010). The IMCC1322 genome ranked first with respect to the number of membrane transporter ORFs per genome size (Table 9), and principal component analysis indicated that strain IMCC1322 was an outlier, with other PR-harboring genomes (Fig. 12). However, no increase of cell numbers under constant light vs. constant dark conditions was apparent (Fig. 5A). This indicated that the membrane potential or ATP generation via light-dependent proton pumping may not involve ABC-transporters or TRAPs in strain IMCC1322. As shown below, IMCC1322 cells were able to metabolize a variety of organic compounds, including C_1 compounds, di-/tri-carboxylic acids, amino acids, sugars, sugar alcohols/polyols, sulfonium compounds, and amines (Table 10 and Table 11). However, light-dependent proton pumping did not affect the growth yields of strain

IMCC1322 regardless of the nutrient concentration (Fig. 5A), even though the PR of IMCC1322 was functional (Fig. 4). In fact, cell numbers in cultures grown in constant darkness were slightly higher in the presence of high nutrient levels [1× mPYC (DD) on day 10] than cultures grown under constant illumination (Fig. 5A).

8. *Bacterial Response to Carbon Monoxide*

In conjunction with light-driven growth enhancement, the presence of a putative CODH was evaluated in strain IMCC1322. The growth of CO-treated cultures, with or without light exposure, was inhibited compared with growth under heterotrophic conditions (0.05× mPYC or 0.01× mPYC) (Fig. 5B). Up to 20% (v/v) CO in the incubation tube headspace was used, and we hypothesized that such high concentrations might generate conditions that are too harsh for the cells to tolerate. Indeed, cell growth was inhibited in 0.01× mPYC medium with CO (DD+CO). However, light exposure of the above culture (LL+CO) partially reversed the effect of CO-induced growth inhibition (Fig. 5B). CO is a potent antibacterial agent, as it binds strongly and readily to respiratory

heme-containing proteins (Chin BY and Otterbein LE, 2009). Blockage of the respiratory system by CO results in the shutdown of ATP-dependent membrane potential; however, this effect can be attenuated by the light-driven proton pump PR, as PR functions under oxygen-depleted conditions, or after treatment with the respiratory inhibitor azide (Walter JM *et al.*, 2007). Unlike strict CO_2-fixing anaerobes that are sulfitogenic, acetogenic, methanogenic, or hydrogenogenic, aerobic-type CO oxidizers are regarded as carboxydotrophs that can survive moderately higher levels of CO (>1% CO). Furthermore, carboxydovores can utilize CO (≤ 1000 ppm) as an energy source, but do not tolerate elevated CO concentrations (King GM and Weber CF, 2007). The solubility of CO in seawater (19.00‰ chlorinity) is 1.825% (v/v) at 25 °C and 1 atm (Douglas E, 1967), which is equivalent to 746 μmol/l (18.25 ml of dissolved CO per 1 l of seawater) for 100% CO in the head space at a standard ambient temperature and pressure (concentration of CO = 1.145 g/l at 25 °C and 1 atm). Assuming that the seawater-based mPYC medium used in the current study contained 20% CO in the head space, the concentration of dissolved CO in the aqueous fraction would be very high, i.e., 149 μmol/l. Likewise, the maximum concentrations of dissolved CO tolerated by carboxydotrophs (> 1%) and carboxydovores (< 1000 ppm) in seawater

are > 7.46 μmol/l and < 746 nmol/l, respectively, as previously determined (King GM and Weber CF, 2007). This is much higher than the standard diurnal CO concentrations at the sea surface, i.e., approximately 1.78–7.08 nmol/l (equatorial Pacific) or 81.8 fmol/l–8.59 nmol/l (Atlantic and Pacific) (Ohta K, 1997). Upon light exposure and at a relative nutrient limitation (LL+CO), strain IMCC1322 was able to tolerate a concentration of CO that was three orders of magnitude higher than that tolerated in the darkness (Fig. 5B). We speculated that this aerobic heterotroph might be able to utilize nanomolar concentrations of CO, similarly to other marine organisms that produce aerobic-type carbon monoxide dehydrogenases (Cox or CODH). The complete genome of the marine CO and sulfide oxidizer *Ruegeria pomeroyi* DSS-3 reportedly contains two gene clusters, each containing *coxL*-1 and *coxL*-2 (Moran MA *et al.*, 2004); it also harbors two copies of putative *coxL/cutL* homologues whose functions have not yet been conclusively determined. Form I CoxL (OMP; CoxL in *Oligotropha*, *Mycobacterium*, and *Pseudomonas*) is thought to be mandatory for CO oxidizers, while form II CoxL (BMS; large subunit of CODH in *Bradyrhizobium*, *Mesorhizobium*, and *Sinorhizobium*) is non-essential (King GM and Weber CF, 2007). Two CODH homologues were identified in strain IMCC1322 (Oh HM *et al.*, 2010). Further phylogenetic

analyses were carried out in the current study using the *coxL/cutL* reference sequences from PFAM (PF02738) (data not shown). One homologue (SAR116_2146) is a putative form II *coxL* (BMS) with an AYXGAGR active-site motif (King GM and Weber CF, 2007); the other homologue (SAR116_0095) is a putative *coxL/cutL* gene. SAR116_2163 (*coxS*), SAR116_2164 (*coxL*), and SAR116_2165 (*coxM*) were compared with form II *coxL/cutL* genes from other bacterial genomes (Fig. S6). However, the phylogenetic and comparative genomic approaches used did not reveal whether these two sets of CODH clusters are directly related to CODH activity. Solar radiation generates CO from dissolved organic matter (DOM) in the ocean (Moran MA *et al.*, 2004; Moran MA and Miller WL, 2007; Reisch CR *et al.*, 2011; Yoch DC, 2002), and PR genes are widespread among diverse taxa other than Proteobacteria. Nevertheless, cultured PR-containing bacteria harboring CODH genes should be studied in detail, as shown in Fig. 11B.

9. *Evaluating the Proprietary PR Function by a Light-Emitting Diode (LED) Test*

We determined the spectroscopic characteristics and proton-pumping function of the retinylidene protein PR from strain IMCC1322 (Fig. 4). However, light-enhanced growth response could not be confirmed (Fig. 5), similarly to what has been observed for SAR92 (Stingl U *et al.*, 2007a) and SAR11 (Giovannoni SJ *et al.*, 2005). Consequently, the light illumination sources were checked to address the question of the light-independent growth response of strain IMCC1322. The initial SAR116 cultivation experiments involved a compact fluorescent lamp (CFL) (fluorescent P-type lamp) that had been used in SAR11 and SAR92 studies (Cho JC and Giovannoni SJ, 2004; Giovannoni SJ *et al.*, 2005; Stingl U *et al.*, 2007a). However, since LED as an illumination source has also been reported (Johnson ET *et al.*, 2010; Spring S *et al.*, 2009; Steindler L *et al.*, 2011), we analyzed the CFL and LED spectra (see above).

The CFL spectrum did not show apparent peaks around the wavelength effective for IMCC1322 PR (522 nm) (Fig. 12A) and the singular wavelength of pure green LED was 525.5 nm (Fig. 12B). CFL did not cover the wavelength encompassing the absorption maximum (Fig. 6) of

green-tuned PR (GPR) (λ_{max} = 522 nm) from IMCC1322 (Fig. 4). CFL may well be suited for the analysis of blue-tuned PR (BPR) (λ_{max} = 490 nm) studied in the Sargasso Sea SAR11 groups (Stingl U *et al.*, 2007b) and Hot75m1 (AAK30177) (Man D *et al.*, 2003; Ranaghan MJ *et al.*, 2010). However, the pure green LED illumination (Fig. 6B; λ_{max} = 525.5 nm) did not affect the cultures of strain IMCC1322 grown in constant light or darkness, as shown in Fig. 5A. The same cultural responses were observed for pure green light and CFL.

Ⅳ. Discussion

Strain IMCC1322, the first colony-forming strain from the SAR116 clade, was isolated on conventional heterotrophic agar plates by chance. By contrast, most other SAR116 isolates were cultured using the deliberate dilution-to-extinction method (Connon SA and Giovannoni SJ, 2002; Stingl U *et al.*, 2007b). Strain IMCC1322 belongs to the OCS28 sub-clade, whereas HTCC8037 (Stingl U *et al.*, 2007b) and HIMB100 (Grote J *et al.*, 2011), which were isolated by dilution-to-extinction cultures, belong to the OM25/OCS24 sub-clade of SAR116. *Rhodospirillaceae* and *Acetobacteriaceae* are the closest sister clades of the SAR116 group. The

colony-forming strain IMCC1322 and its completed genome (sequenced from colony-derived genomic DNA) (Oh HM *et al.*, 2010) allowed us to attempt physiological investigations based on its genomic predictions and polyphasic taxonomy, using a SAR116 isolate in addition to its phage isolation (Kang I *et al.*, 2013).

Vibrioid and elongated forms of IMCC1322 cells were observed. Based on microscopic evaluations, they were non-motile. Vibrioids cannot aggregate into larger particles by predation, fecal pellet formation, or marine snow formation (Worden ZA and Not F, 2008). However, upon induction by DNA damage, aging, or appropriate nutrient conditions, spiral IMCC1322 cells could circumvent bacterivory, unless other predators picked them off. Picoplankton (both eukaryotic and prokaryotic) is governed by the viscous forces of seawater columns, rather than inertial forces (Worden ZA and Not F, 2008). Thus, the Reynold's number [R_e = (inertial force)/(viscous force)] of short IMCC1322 cells would be lower than that of long spiral cells; that is, the elongated forms are more prone to be stirred by seawater turbulence than the short vibrioid forms, whose boundary layers are more dominated by the laminar flow than spirals. Because spirals are stirred up more easily by turbulent forces than vibrioids (Purcell EM, 1977), the spiral IMCC1322 cells would sink more

slowly than vibrioids, an advantage of the elongated forms over vibrioids. Free-living spiral IMCC1322 cells may position themselves in the water column via cellular shape changes. High-density IMCC1322 cells formed flocs in mPYC (data not shown), which is why the initial cultivation studies of the IMCC1322 strain were challenging.

Despite the remarkable discovery of PR in SAR86 and its photoheterotrophic potential (Beja O *et al.*, 2000; Beja O *et al.*, 2001), little direct evidence for PR-enhanced marine microbial heterotrophy has been provided to date. The predicted function of PR could not be confirmed by the pioneering axenic culture of a SAR11 isolate, *Candidatus* Pelagibacter ubique HTCC1062 (Giovannoni SJ *et al.*, 2005). *Candidatus* P. ubique HTCC1062 studies indicated PR-mediated ATP generation upon light exposure, but the light-enhanced response was only significant under nutrient starvation (Steindler L *et al.*, 2011), as also observed in another study investigating *Vibrio* sp. strain AND4 (Gomez-Consarnau L *et al.*, 2010). The San Pedro Ocean Time Series (SPOTS) light-impacted microcosm experiment (Schwalbach MS *et al.*, 2005) revealed that the ARISA profiles of SAR116 reflect the light preference of SPOTSAUG01_5m101 (GenBank acc. no. DQ009267) and dark preference by SPOTSAUG01_5m67 (GenBank acc. no. DQ009264). Both

light-impacted ARISA profiles of SAR116 clones matched those of OCS126 (Schwalbach MS *et al.*, 2005). Strain IMCC1322 (from OCS28) is a distant relative of OCS126 (Fig. 1), but such light-regulated changes as cell numbers or OTU numbers were difficult to detect, similarly to what has been reported for SAR11 and SAR86 (Schwalbach MS *et al.*, 2005): appreciable growth enhancement was not apparent for strain IMCC1322 cultured in the light or darkness. The observations made for the light-exposed IMCC1322 culture differed from those of the marine PR-bearing *Flavobacteria* (Gomez-Consarnau L *et al.*, 2007; Gonzalez JM *et al.*, 2008) and *Vibrio* species (Gomez-Consarnau L *et al.*, 2010) that show photoheterotrophic potential. No light-enhanced biomass or cell count increase in IMCC1322 culture was observed, unlike other PR-bearing oligotrophic bacteria including SAR11 (Steindler L *et al.*, 2011) and SAR92 (Stingl U *et al.*, 2007a). PR expressed in *E. coli* catalyzes light-driven proton gradient across the membrane (Walter JM *et al.*, 2007) and light-mediated ATP production (Steindler L *et al.*, 2011), and such light-stimulated cultivation studies are well established for *Dokdonia donghaensis* MED134 (Gomez-Consarnau L *et al.*, 2007), *Polaribacter* sp. MED152 (Gonzalez JM *et al.*, 2008), and *Vibrio* sp. AND4 (Gomez-Consarnau L *et al.*, 2010).

Analyses of various culture responses to combinations of light, nutrient concentrations, and headspace CO content (Fig. 5), and DMSP supplementation (Fig. 11 and Table 2) suggested that strain IMCC1322 could be a model species for investigating biogeochemical processes occurring at the ocean surface. In strain IMCC1322, PR probably functions as a coping mechanism against starvation (nutrient limitation) or against shutdown of oxidative phosphorylation (e.g., under anoxic conditions or in the presence of CO, which binds heme proteins involved in oxidative phosphorylation). However, the growth of IMCC1322 cells was not enhanced under typical aerobic conditions with light exposure, regardless of the presence of organic nutrients in the medium. Nutrient limitation outweighed light-enhanced responses of strain IMCC1322. In the current study, we did not observe light-enhanced biomass production (determined by cell counting) under nutrient-limited conditions; a slight biomass increase was observed in cultures grown constantly in the dark, even with LED illumination as an alternative light source. LED is used as an illumination source for GPR for enhanced microbial electricity production (Johnson ET *et al.*, 2010) and as a light source in a transcriptome study of SAR11, (Steindler L *et al.*, 2011) despite the fact that improved biohydrogen production by GPR was reported with CFL as

a light source (Kim JY *et al.*, 2012). In the current study, the used light sources did not exert any appreciable effect on the phototrophic potential of strain IMCC1322 in liquid culture.

The growth of IMCC1322 cells was almost completely abolished in a low-nutrient medium in the dark with 20% CO in the headspace of culture vessels (DD+CO). However, light exposure (LL+CO) induced bacterial cell numbers. Based on this observation, we propose that PR may help SAR116 bacteria to cope with anoxic conditions or the inhibition of heme protein function. Two CODH gene clusters on the IMCC1322 genome may be redundant at such high CO concentrations (20% air/head space), but the possibility that aerobic CODH may be linked to the consumption of nanomolar CO at a typical sea surface cannot be excluded, as has been proposed for other marine heterotrophic bacteria (Moran MA *et al.*, 2004; Moran MA and Miller WL, 2007; Reisch CR *et al.*, 2011).

Based on the performed genomic and biochemical analyses, in addition to basic cultivation efforts, we conclude that strain IMCC1322 is metabolically adaptable to diverse nutrients, and contains many genes for the utilization of carbon, nitrogen, phosphorous, and sulfur compounds, as well as a wide variety of genes encoding ABC-type and ATP-independent

metabolite transporters. The isolation and cultivation of strain IMCC1322 supports the role of the SAR116 group as metabolic generalists among Alphaproteobacteria. The current study provides substantial evidence for the potential role of the SAR116 group in the marine sea surface environment. SAR116 members (including strain IMCC1322) may utilize CO and DMSP via aerobic respiration, similarly to many other marine bacteria (Moran MA *et al.*, 2004; Moran MA and Miller WL, 2007). Marine algae produce DOM, which includes DMSP, by utilizing sunlight at the sea surface (Moran MA *et al.*, 2004; Moran MA and Miller WL, 2007; Reisch CR *et al.*, 2011; Yoch DC, 2002); CO is released from DOM in the seawater by solar radiation (Ohta K, 1997; Stubbins A *et al.*, 2006; Zafiriou OC *et al.*, 2003). In the current study, strain IMCC1322 was found to contain genes encoding PR, DMSP enzymes, two copies of CODH, and proteins controlling many other biochemical processes. These features demonstrate that the genome of strain IMCC1322 is well adapted to the upper sea surface environment. Based on the observed simple morphological changes of ICC1322 cells from vibrioid to spiral, we speculate that strain IMCC1322 would thrive in a euphotic region of the sea surface.

De Long and Yayanos (Delong EF and Yayanos AA, 1986) argued for

the involvement of PUFAs in the maintenance of optimal membrane fluidity and function of deep-sea bacteria in the abyssal food webs. Groups of marine PUFA-producing bacteria exhibit a phylogenetic linkage centered on two distinct lineages: marine Gammaproteobacteria and *Cytophaga-Flavobacterium-Bacteroidetes* (CFB) groups (Nichols DS, 2003). PUFAs have been found in a myxobacterial group (Iizuka T *et al.*, 2003) and halotolerant *Roseobacter* isolates (Lee OO *et al.*, 2007). Marine *Bacteroidetes* reportedly produce AA and eicosapentaenoic acid ($C_{20:5}\omega$3,6,9,12,15c) via the secondary lipid biosynthetic systems for PUFAs (Shulse CN and Allen EE, 2011). The genes responsible for *de novo* bacterial PUFA biosynthesis (designated *pfaEABCD* or type I FAS/PKS gene cluster) (Shulse CN and Allen EE, 2011) were not identified in the IMCC1322 genome. It may be argued that the bacterium may utilize a novel biosynthetic pathway for PUFA production; however, it is more likely that genes for secondary lipid and AA synthesis are poorly annotated and interspersed throughout the genome. To the best of our knowledge, strain IMCC1322 is the first identified PUFA-producer from the sea surface environment in the SAR116 group. The phylogenetic, biochemical, and chemotaxonomic characteristics of *Candidatus* P. marinum IMCC1322 from the sub-group OCS28 of SAR116 of

Alphaproteobacteria are summarized and proposed below.

Proposition of *Candidatus* Puniceispirillum marinum gen. nov. sp nov.

Candidatus Puniceispirillum marinum (L. neut. adj. *marinum*, of or belonging to the sea, marine)

Description is the same as the genus. At stationary phase cells were of sizes 2.01 μm long (σ= ±0.546 μm, n = 30) and 0.375 μm wide (σ = ±0.0420 μm, n=30). Log-phase cells are vibroids and were 2.72 μm long (σ= ±0.581 μm, n = 30) and 0.377 μm wide (σ = ±0.0416 μm, n=30) but mitomycin-C-induced spiral forms were 6.03 μm long (σ=±0.540 μm, n = 30) and 0.319 μm wide (σ = ±0.0510 μm, n=30). Growth occurs at 18.1 ~ 32.3 °C, and optimum growth was at 25.5 °C. The pH for growth are 6.0 ~ 9.6; optimum growth occurs at pH 7.0–7.4. Growth occurs between 60% ~ 115% salt level of sea water (w/w) and optimum salinity range is 80 ~ 100 % sea salt level. Nitrate reduction and oxidase are negative, but catalase is positive. Indole production, glucose fermentation, arginine dihydrolase, urease, esculin hydrolysis, gelatinase, PNPG (β-galactosidase) are negative for IMCC1322, while esterase (C4), esterase lipase (C8), leucine

arylamidase, valine arylamidase, and trypsin are positive. Alkaline phosphatase, acid phosphatase, lipase (C14), cystine arylamidase, α-chymotrypsin, naphthol-AS-BI-phosphohydrolase, α-galactosidase, β-galactosidase, β-glucuronidase, α-glucosidase, β-glucosidase, N-acetyl-β-glucosaminidase are negative. Starch hydrolysis is negative. Carbon sources utilization patterns are described in the text and Table 1 and these included C_1 compounds; formic acid, methanol, and methanesulfonic acid. Carbon source tests for DL-glyceraldehyde, D-xylose, sodium gluconate, D-cellobiose, melibiose, D-maltose monohydrate, D-melezitose, Adonitol, L-arabitol, xylitol, D-mannitol, D-sorbitol, glycerol, methanol, formic acid, DL-methionine, DL-methionine methylsulfonium chloride, DMSP, N,N-dimethylglycine, betaine hydrochloride, choline chloride, potassium acetate, pimelic acid, malonic acid, sodium citrate (trisodium salt), acetamide, DL-glutamine, DL-aspartic acid, L-histidine, L-arginine monohydrochloride, DL-lysine dihydrochloride, glycine, DL-alanine, L-leucine, and DL-threonine are positive. D-Glucosamine hydrochloride, D-lactose monohydrate, D-Trehalose, and fumaric acid are negative for carbon source tests for IMCC1322. Weakly positive results for carbon sources tested included L-rhamnose, D-fructose, D-galactose, dextrose, D-mannose, D-glucuronic acid sodium

salt monohydrate, D-raffinose, meso-erythritol, myo-inositol, ethylene glycol, methanesulfonic acid sodium salt (MSA), 2-aminoethanesulfonic acid (taurine), dimethylsulfoxide (DMSO), 2,6-diaminopimelic acid, trimethylamine, DL-carnitine hydrochloride, sodium salicylate, sodium pyruvate, succinic acid, glutaric acid, adipic acid, L-glutamic acid monosodium salt hydrate, L-ornithine monohydrochloride, DL-proline, and DL-serine. The predominant fatty acids are monounsaturated fatty acids including $C_{16:1}$ (49.78%), $C_{18:1}$ (39.98%), plus polyunsaturated fatty acid $C_{20:4}$ (n-6) (1.02%). The DNA G+C content of the species is 48.85 mol% (HPLC method). The type strain of *Puniceispirillum marinum* is IMCC1322 isolated at a depth of 50 m from surface water of the East Sea of Korea.

참고문헌

Acinas SG, Anton J, and Rodriguez-Valera F. 1999. Diversity of free-living and attached bacteria in offshore Western Mediterranean waters as depicted by analysis of genes encoding 16S rRNA. *Applied and environmental microbiology* **65**, 514-522.

Althoff K, Schütt C, Steffen R, Batel R, and Müller WEG. 1998. Evidence for a symbiosis between bacteria of the genus *Rhodobacter* and the marine sponge *Halichondria panicea*: harbor also for putatively toxic bacteria? *Marine Biology* **130**, 529-536.

Béjà O, Suzuki MT, Koonin EV, Aravind L, Hadd A, Nguyen LP, Villacorta R, Amjadi M, Garrigues C, Jovanovich SB, Feldman RA, and DeLong EF. 2000. Construction and analysis of bacterial artificial chromosome libraries from a marine microbial assemblage. *Environmental Microbiology* **2**, 516-529.

Balashov SP and Lanyi JK. 2007. Xanthorhodopsin: Proton pump with a carotenoid antenna. *Cell Mol Life Sci* **64**, 2323-2328.

Bano N and Hollibaugh JT. 2002a. Phylogenetic composition of bacterioplankton assemblages from the Arctic Ocean. *Applied and environmental microbiology* **68**, 505-518.

Bano N and Hollibaugh JT. 2002b. Phylogenetic Composition of Bacterioplankton Assemblages from the Arctic Ocean. *Appl. Environ. Microbiol.* **68**, 505-518.

Beja O, Aravind L, Koonin EV, Suzuki MT, Hadd A, Nguyen LP, Jovanovich SB, Gates CM, Feldman RA, Spudich JL, Spudich EN, and DeLong EF. 2000. Bacterial rhodopsin: evidence for a new type of phototrophy in the sea. *Science* **289**, 1902-1906.

Beja O, Spudich EN, Spudich JL, Leclerc M, and DeLong EF. 2001. Proteorhodopsin phototrophy in the ocean. *Nature* **411**, 786-789.

Bernhard MF, Dagmar W, Mikhail VZ, Peter B, and Rudolf A. 2005. Molecular

identification of picoplankton populationsin contrasting waters of the Arabian Sea. *Aquatic Microbial Ecology* **39**, 145-157.

Bourne DG and Munn CB. 2005. Diversity of bacteria associated with the coral Pocillopora damicornis from the Great Barrier Reef. *Environmental Microbiology* **7**, 1162-1174.

Britschgi TB and Giovannoni SJ. 1991. Phylogenetic analysis of a natural marine bacterioplankton population by rRNA gene cloning and sequencing. *Applied and environmental microbiology* **57**, 1707-1713.

Brown MV, Schwalbach MS, Hewson I, and Fuhrman JA. 2005. Coupling 16S-ITS rDNA clone libraries and automated ribosomal intergenic spacer analysis to show marine microbial diversity: development and application to a time series. *Environmental Microbiology* **7**, 1466-1479.

Campbell BJ, Yu L, Straza TRA, and Kirchman DL. 2009. Temporal changes in bacterial rRNA and rRNA genes in Delaware (USA) coastal waters. *Aquat Microb Ecol* **57**, 123-135.

Chin BY and Otterbein LE. 2009. Carbon monoxide is a poison... to microbes! CO as a bactericidal molecule. *Current opinion in pharmacology* **9**, 490-500.

Cho JC and Giovannoni SJ. 2004. Cultivation and growth characteristics of a diverse group of oligotrophic marine Gammaproteobacteria. *Applied and environmental microbiology* **70**, 432-440.

Cho JC and Giovannoni SJ. 2006. *Pelagibaca bermudensis* gen. nov., sp. nov., a novel marine bacterium within the *Roseobacter* clade in the order *Rhodobacterales*. *International journal of systematic and evolutionary microbiology* **56**, 855-859.

Choo YJ, Lee K, Song J, and Cho JC. 2007. *Puniceicoccus vermicola* gen. nov., sp. nov., a novel marine bacterium, and description of *Puniceicoccaceae* fam. nov., *Puniceicoccales* ord. nov., *Opitutaceae* fam. nov., *Opitutales* ord. nov. and *Opitutae* classis nov. in the phylum '*Verrucomicrobia*'. *International journal of systematic and evolutionary microbiology* **57**, 532-537.

Connon SA and Giovannoni SJ. 2002. High-throughput methods for culturing microorganisms in very-low-nutrient media yield diverse new marine isolates. *Applied and environmental microbiology* **68**, 3878-3885.

Delong EF and Yayanos AA. 1986. Biochemical function and ecological significance of novel bacterial lipids in deep-sea procaryotes. *Applied and environmental microbiology* **51**, 730-737.

Douglas E. 1967. Carbon monoxide solubilities in sea water. *The Journal of Physical Chemistry* **71**, 1931-1933.

Dupont CL, Rusch DB, Yooseph S, Lombardo MJ, Richter RA, Valas R, Novotny M, Yee-Greenbaum J, Selengut JD, Haft DH, Halpern AL, Lasken RS, Nealson K, Friedman R, and Venter JC. 2012. Genomic insights to SAR86, an abundant and uncultivated marine bacterial lineage. *The ISME journal* **6**, 1186-1199.

Finn RD, Tate J, Mistry J, Coggill PC, Sammut SJ, Hotz HR, Ceric G, Forslund K, Eddy SR, Sonnhammer EL, and Bateman A. 2008. The Pfam protein families database. *Nucleic acids research* **36**, D281-288.

Gallagher JM, Carton MW, Eardly DF, and Patching JW. 2004. Spatio temporal variability and diversity of water column prokaryotic communities in the eastern North Atlantic. *FEMS microbiology ecology* **47**, 249-262.

Giovannoni SJ, Bibbs L, Cho JC, Stapels MD, Desiderio R, Vergin KL, Rappe MS, Laney S, Wilhelm LJ, Tripp HJ, Mathur EJ, and Barofsky DF. 2005. Proteorhodopsin in the ubiquitous marine bacterium SAR11. *Nature* **438**, 82-85.

Giovannoni SJ, Britschgi TB, Moyer CL, and Field KG. 1990. Genetic diversity in Sargasso Sea bacterioplankton. *Nature* **345**, 60-63.

Giovannoni SJ and Rappé MS. (2000) Evolution, Diversity, and Molecular Ecology of Marine Prokaryotes. In Kirchman, DLE (ed.), *Microbial Ecology of the Oceans.* . Wiley-Liss New York, pp. 47-84.

Gomez-Consarnau L, Akram N, Lindell K, Pedersen A, Neutze R, Milton DL, Gonzalez JM, and Pinhassi J. 2010. Proteorhodopsin phototrophy promotes survival of marine bacteria during starvation. *PLoS biology* **8**, e1000358.

Gomez-Consarnau L, Gonzalez JM, Coll-Llado M, Gourdon P, Pascher T, Neutze R, Pedros-Alio C, and Pinhassi J. 2007. Light stimulates growth of proteorhodopsin-containing marine Flavobacteria. *Nature* **445**, 210-213.

Gonzalez JM, Fernandez-Gomez B, Fernandez-Guerra A, Gomez-Consarnau L, Sanchez O, Coll-Llado M, Del Campo J, Escudero L, Rodriguez-Martinez R, Alonso-Saez L, Latasa M, Paulsen I, Nedashkovskaya O, Lekunberri I, Pinhassi J, and Pedros-Alio C. 2008. Genome analysis of the proteorhodopsin-containing marine bacterium Polaribacter sp. MED152 (Flavobacteria). *Proceedings of the National Academy of Sciences of the United States of America* **105**, 8724-8729.

Gonzalez JM, Simo R, Massana R, Covert JS, Casamayor EO, Pedros-Alio C, and Moran MA. 2000. Bacterial Community Structure Associated with a Dimethylsulfoniopropionate-Producing North Atlantic Algal Bloom. *Appl. Environ. Microbiol.* **66**, 4237-4246.

Grote J, Bayindirli C, Bergauer K, Carpintero de Moraes P, Chen H, D'Ambrosio L, Edwards B, Fernandez-Gomez B, Hamisi M, Logares R, Nguyen D, Rii YM, Saeck E, Schutte C, Widner B, Church MJ, Steward GF, Karl DM, Delong EF, Eppley JM, Schuster SC, Kyrpides NC, and Rappe MS. 2011. Draft genome sequence of strain HIMB100, a cultured representative of the SAR116 clade of marine Alphaproteobacteria. *Standards in genomic sciences* **5**, 269-278.

Huber JA, Johnson HP, Butterfield DA, and Baross JA. 2006. Microbial life in ridge flank crustal fluids. *Environmental Microbiology* **8**, 88-99.

Iizuka T, Jojima Y, Fudou R, Hiraishi A, Ahn JW, and Yamanaka S. 2003. Plesiocystis pacifica gen. nov., sp. nov., a marine myxobacterium that contains dihydrogenated menaquinone, isolated from the Pacific coasts of Japan. *International journal of systematic and evolutionary microbiology* **53**, 189-195.

Johnson ET, Baron DB, Naranjo B, Bond DR, Schmidt-Dannert C, and Gralnick JA. 2010. Enhancement of survival and electricity production in an engineered bacterium by light-driven proton pumping. *Applied and environmental microbiology* **76**, 4123-4129.

Jorgensen JH, Turnidge JD, and Washington JA. (1999) Antibacterial susceptibility tests : dilution and disk diffusion methods. In Murray, PR, Baron, EJ, Pfaller, MA, Tenover, FC, and Yolken, RH (eds.), *Manual of Clinical Microbiology*. American Society for Microbiology, Washington, DC, pp. 1526-1543.

Juliette NT, Jane LH, Peter W, and Mikhail VZ. 2006. Bacterioplankton composition in the Scotia Sea, Antarctica, during the austral summer of 2003. *Aq. Microb. Ecol.* **45**, 229-235.

Kamke J, Taylor MW, and Schmitt S. 2010. Activity profiles for marine sponge-associated bacteria obtained by 16S rRNA vs 16S rRNA gene comparisons. *ISME J* **4**, 498-508.

Kan J, Evans SE, Chen F, and Suzuki MT. 2008. Novel estuarine bacterioplankton in rRNA operon libraries from the Chesapeake Bay. *Aquat Microb Ecol* **51**, 55-66.

Kang I, Oh HM, Kang D, and Cho JC. 2013. Genome of a SAR116 bacteriophage shows the prevalence of this phage type in the oceans. *Proceedings of the National Academy of Sciences of the United States of America* **110**, 12343-12348.

Kim JY, Jo BH, Jo Y, and Cha HJ. 2012. Improved production of biohydrogen in light-powered Escherichia coli by co-expression of proteorhodopsin and heterologous hydrogenase. *Microbial cell factories* **11**, 2.

Kim SY, Waschuk SA, Brown LS, and Jung KH. 2008. Screening and characterization of proteorhodopsin color-tuning mutations in Escherichia coli with endogenous retinal synthesis. *Biochimica et biophysica acta* **1777**, 504-513.

King GM and Weber CF. 2007. Distribution, diversity and ecology of aerobic CO-oxidizing bacteria. *Nat Rev Microbiol* **5**, 107-118.

Lami R, Ghiglione JF, Desdevises Y, West NJ, and Lebaron P. 2009. Annual patterns of presence and activity of marine bacteria monitored by 16S rDNA-16S rRNA fingerprints in the coastal NW Mediterranean Sea. *Aquat Microb Ecol* **54**, 199-210.

Lau WWY and Armbrust EV. 2006. Detection of glycolate oxidase gene glcD diversity among cultured and environmental marine bacteria. *Environmental Microbiology* **8**, 1688-1702.

Lee OO, Tsoi MM, Li X, Wong PK, and Qian PY. 2007. *Thalassococcus halodurans* gen. nov., sp. nov., a novel halotolerant member of the *Roseobacter* clade isolated from the marine sponge *Halichondria panicea* at Friday Harbor, USA. *International journal of systematic and evolutionary microbiology* **57**, 1919-

1924.

Ludwig W, Strunk O, Westram R, Richter L, Meier H, Yadhukumar, Buchner A, Lai T, Steppi S, Jobb G, Forster W, Brettske I, Gerber S, Ginhart AW, Gross O, Grumann S, Hermann S, Jost R, Konig A, Liss T, Lussmann R, May M, Nonhoff B, Reichel B, Strehlow R, Stamatakis A, Stuckmann N, Vilbig A, Lenke M, Ludwig T, Bode A, and Schleifer KH. 2004. ARB: a software environment for sequence data. *Nucleic acids research* **32**, 1363-1371.

Macleod RA. 1965. The Question of the Existence of Specific Marine Bacteria. *Bacteriological reviews* **29**, 9-24.

Man D, Wang W, Sabehi G, Aravind L, Post AF, Massana R, Spudich EN, Spudich JL, and Beja O. 2003. Diversification and spectral tuning in marine proteorhodopsins. *The EMBO journal* **22**, 1725-1731.

Minnikin DE, O'Donnell AG, Goodfellow M, Alderson G, Athalye M, Schaal A, and Parlett JH. 1984. An integrated procedure for the extraction of bacterial isoprenoid quinones and polar lipids. *Journal of Microbiological Methods* **2**, 233-241.

Moran MA, Buchan A, Gonzalez JM, Heidelberg JF, Whitman WB, Kiene RP, Henriksen JR, King GM, Belas R, Fuqua C, Brinkac L, Lewis M, Johri S, Weaver B, Pai G, Eisen JA, Rahe E, Sheldon WM, Ye W, Miller TR, Carlton J, Rasko DA, Paulsen IT, Ren Q, Daugherty SC, Deboy RT, Dodson RJ, Durkin AS, Madupu R, Nelson WC, Sullivan SA, Rosovitz MJ, Haft DH, Selengut J, and Ward N. 2004. Genome sequence of Silicibacter pomeroyi reveals adaptations to the marine environment. *Nature* **432**, 910-913.

Moran MA and Miller WL. 2007. Resourceful heterotrophs make the most of light in the coastal ocean. *Nat Rev Microbiol* **5**, 792-800.

Morris RM, Vergin KL, Cho JC, Rappe MS, Carlson CA, and Giovannoni SJ. 2005. Temporal and spatial response of bacterioplankton lineages to annual convective overturn at the Bermuda Atlantic Time-series Study site. *Limnol Oceanogr* **50**, 1687-1696.

Mou X, Hodson RE, and Moran MA. 2007. Bacterioplankton assemblages transforming dissolved organic compounds in coastal seawater. *Env. Microbiol.*

9, 2025-2037.

Mullins TD, Britschgi TB, Krest RL, and Giovannoni SJ. 1995. Genetic Comparisons Reveal the Same Unknown Bacterial Lineages in Atlantic and Pacific Bacterioplankton Communities. *Limnology and Oceanography* **40**, 148-158.

Nelson CE, Alldredge AL, McCliment EA, Amaral-Zettler LA, and Carlson CA. 2011. Depleted dissolved organic carbon and distinct bacterial communities in the water column of a rapid-flushing coral reef ecosystem. *ISME J* **5**, 1374-1387.

Nichols DS. 2003. Prokaryotes and the input of polyunsaturated fatty acids to the marine food web. *FEMS Microbiol Lett* **219**, 1-7.

Noble RT and Fuhrman JA. 1998. Use of SYBR Green I for rapid epifluorescence counts of marine viruses and bacteria. *Aquat Microb Ecol* **14**, 113-118.

Oh HM, Kang I, Lee K, Jang Y, Lim SI, and Cho JC. 2011. Complete genome sequence of strain IMCC9063, belonging to SAR11 subgroup 3, isolated from the Arctic Ocean. *Journal of bacteriology* **193**, 3379-3380.

Oh HM, Kwon KK, Kang I, Kang SG, Lee JH, Kim SJ, and Cho JC. 2010. Complete genome sequence of "*Candidatus* Puniceispirillum marinum" IMCC1322, a representative of the SAR116 clade in the *Alphaproteobacteria*. *Journal of bacteriology* **192**, 3240-3241.

Ohta K. 1997. Diurnal variations of carbon monoxide concentration in the Equatorial Pacific upwelling region. *Oceanographic Literature Review* **44**, 1258.

Poretsky RS, Sun S, Mou X, and Moran MA. 2010. Transporter genes expressed by coastal bacterioplankton in response to dissolved organic carbon. *Environmental Microbiology* **12**, 616-627.

Pruesse E, Quast C, Knittel K, Fuchs BM, Ludwig W, Peplies J, and Glockner FO. 2007. SILVA: a comprehensive online resource for quality checked and aligned ribosomal RNA sequence data compatible with ARB. *Nucleic acids research* **35**, 7188-7196.

Purcell EM. 1977. Life at low Reynolds number. *American Journal of Physics* **45**, 3-11.

Rachel TN and Jed AF. 1998. Use of SYBR Green I for rapid epifluorescence counts of marine viruses and bacteria. *Aquat Microb Ecol* **14**, 113-118.

Ranaghan MJ, Shima S, Ramos L, Poulin DS, Whited G, Rajasekaran S, Stuart JA,

Albert AD, and Birge RR. 2010. Photochemical and thermal stability of green and blue proteorhodopsins: implications for protein-based bioelectronic devices. *The journal of physical chemistry. B* **114**, 14064-14070.

Rappé MS, Kemp PF, and Giovannoni SJ. 1997. Phylogenetic diversity of marine coastal picoplankton 16s rRNA genes cloned from the continental shelf off Cape Hatteras, North Carolina. *Limnology and Oceanography* **42**, 811-826.

Rappe MS, Vergin K, and Giovannoni SJ. 2000. Phylogenetic comparisons of a coastal bacterioplankton community with its counterparts in open ocean and freshwater systems. *FEMS microbiology ecology* **33**, 219-232.

Reasoner DJ and Geldreich EE. 1985. A new medium for the enumeration and subculture of bacteria from potable water. *Applied and environmental microbiology* **49**, 1-7.

Reisch CR, Moran MA, and Whitman WB. 2011. Bacterial Catabolism of Dimethylsulfoniopropionate (DMSP). *Frontiers in microbiology* **2**, 172.

Sabehi G, Loy A, Jung K-H, Partha R, Spudich JL, Isaacson T, Hirschberg J, Wagner M, and Beja O. 2005. New Insights into Metabolic Properties of Marine Bacteria Encoding Proteorhodopsins. *PLoS biology* **3**, e273.

Schäfer H, Servais P, and Muyzer G. 2000. Successional changes in the genetic diversity of a marine bacterial assemblage during confinement. *Archives of Microbiology* **173**, 138-145.

Schwalbach M, S. , Brown M, and Fuhrman JA. 2005. Impact of light on marine bacterioplankton community structure. *Aq. Microb. Ecol.* **39**, 235-245.

Schwalbach MS, Brown M, and Fuhrman JA. 2005. Impact of light on marine bacterioplankton community structure. *Aquat Microb Ecol* **39**, 235-245.

Shaw AK, Halpern AL, Beeson K, Tran B, Venter JC, and Martiny JBH. 2008. It's all relative: ranking the diversity of aquatic bacterial communities. *Environmental Microbiology* **10**, 2200-2210.

Shulse CN and Allen EE. 2011. Widespread occurrence of secondary lipid biosynthesis potential in microbial lineages. *PloS one* **6**, e20146.

Spring S, Lunsdorf H, Fuchs BM, and Tindall BJ. 2009. The photosynthetic apparatus and its regulation in the aerobic gammaproteobacterium

Congregibacter litoralis gen. nov., sp. nov. *PloS one* **4**, e4866.

Steindler L, Schwalbach MS, Smith DP, Chan F, and Giovannoni SJ. 2011. Energy starved Candidatus Pelagibacter ubique substitutes light-mediated ATP production for endogenous carbon respiration. *PloS one* **6**, e19725.

Stingl U, Desiderio RA, Cho JC, Vergin KL, and Giovannoni SJ. 2007a. The SAR92 clade: an abundant coastal clade of culturable marine bacteria possessing proteorhodopsin. *Applied and environmental microbiology* **73**, 2290-2296.

Stingl U, Tripp HJ, and Giovannoni SJ. 2007b. Improvements of high-throughput culturing yielded novel SAR11 strains and other abundant marine bacteria from the Oregon coast and the Bermuda Atlantic Time Series study site. *The ISME journal* **1**, 361-371.

Stubbins A, Uher G, Law CS, Mopper K, Robinson C, and Upstill-Goddard RC. 2006. Open-ocean carbon monoxide photoproduction. *Deep Sea Research Part II: Topical Studies in Oceanography* **53**, 1695-1705.

Sunagawa S, Woodley CM, and Medina M. 2010. Threatened Corals Provide Underexplored Microbial Habitats. *PLoS ONE* **5**, e9554.

Suzuki MT, Béja O, Taylor LT, and DeLong EF. 2001. Phylogenetic analysis of ribosomal RNA operons from uncultivated coastal marine bacterioplankton. *Environmental Microbiology* **3**, 323-331.

Swofford D. 2002 *PAUP*: phylogenetic analysis using parsimony, version 4.0b10*. Sinauer Associates, Sunderland, Mass.

Treusch AH, Vergin KL, Finlay LA, Donatz MG, Burton RM, Carlson CA, and Giovannoni SJ. 2009. Seasonality and vertical structure of microbial communities in an ocean gyre. *The ISME journal* **3**, 1148-1163.

Venter JC, Remington K, Heidelberg JF, Halpern AL, Rusch D, Eisen JA, Wu D, Paulsen I, Nelson KE, Nelson W, Fouts DE, Levy S, Knap AH, Lomas MW, Nealson K, White O, Peterson J, Hoffman J, Parsons R, Baden-Tillson H, Pfannkoch C, Rogers YH, and Smith HO. 2004. Environmental genome shotgun sequencing of the Sargasso Sea. *Science* **304**, 66-74.

Vergin KL, Rappe MS, and Giovannoni SJ. 2001. Streamlined method to analyze 16S rRNA gene clone libraries. *BioTechniques* **30**, 938-940, 943-934.

Walsh DA, Zaikova E, Howes CG, Song YC, Wright JJ, Tringe SG, Tortell PD, and Hallam SJ. 2009. Metagenome of a Versatile Chemolithoautotroph from Expanding Oceanic Dead Zones. *Science (New York, N.Y)* **326**, 578-582.

Walter JM, Greenfield D, Bustamante C, and Liphardt J. 2007. Light-powering *Escherichia coli* with proteorhodopsin. *Proceedings of the National Academy of Sciences of the United States of America* **104**, 2408-2412.

Wang WW, Sineshchekov OA, Spudich EN, and Spudich JL. 2003. Spectroscopic and photochemical characterization of a deep ocean proteorhodopsin. *The Journal of biological chemistry* **278**, 33985-33991.

West NJ, Obernosterer I, Zemb O, and Lebaron P. 2008. Major differences of bacterial diversity and activity inside and outside of a natural iron-fertilized phytoplankton bloom in the Southern Ocean. *Environmental Microbiology* **10**, 738-756.

Worden ZA and Not F. (2008) Ecology and diversity of picoeukaryotes. In Kirchman, DLE (ed.), *Microbial Ecology of the Oceans, 2nd edition*. John Wiley & Sons, Inc., New York, pp. 159-205.

Yeung CW, Lee K, Whyte LG, and Greer CW. 2010. Microbial community characterization of the Gully: a marine protected area. *Canadian Journal of Microbiology* **56**, 421-431.

Yoch DC. 2002. Dimethylsulfoniopropionate: Its Sources, Role in the Marine Food Web, and Biological Degradation to Dimethylsulfide. *Applied and environmental microbiology* **68**, 5804-5815.

Zafiriou OC, Andrews SS, and Wang W. 2003. Concordant estimates of oceanic carbon monoxide source and sink processes in the Pacific yield a balanced global "blue-water" CO budget. *Global Biogeochemical Cycles* **17**.

Zubkov MV, Fuchs BM, Archer SD, Kiene RP, Amann R, and Burkill PH. 2002. Rapid turnover of dissolved DMS and DMSP by defined bacterioplankton communities in the stratified euphotic zone of the North Sea. *Deep Sea Research Part II: Topical Studies in Oceanography* **49**, 3017-3038.

Table 1. Predicted metabolic pathways from finished genome of IMCC1322

Pathway or Functional Genes	Predicted
Retinal biosynthesis (for PR)	+
CO oxidation	+
CO_2 fixation	-
Methanol Oxidation to formaldehyde	-
Formaldehyde and formate assimilation	+
Serine pathway for methylotrophy	+
RuMP pathway for methylotrophy	-
DMSP demethylation	+
DMSP-cleavage enzymes	+
Methanesulfonate Oxidation	+
DMSO reduction	+
Assimilatory sulfate reduction	+
Nitrogen metabolism	-
Biosynthesis of 20 amino acids	+
Biotin metabolism	-
Folate biosynthesis	+
Nicotinate and nicotinamide metabolism	+
Pantothenate and CoA biosynthesis	+
Vitamin B6 metabolism	+
Riboflavin metabolism	+
Thiamine metabolism	+
Porphyrin and vitamin B12	+
Ubiquinone	+

Table 2. Candidate DMSP utilizing genes from IMCC1322.

All proteins from IMCC1322 genomic information were hmmer3-searched against bacterial DMSP utilizing genes reviewed by Reische et. al (Reisch CR *et al.*, 2011); dddD, dddL, dddP, dddY, dddQ, dddW, and dmdA

GENE	Locus	Description	PFAM ID's
dddP	SAR116_1427	peptidase M24 (EC:3.4.13.9)	Peptidase_M24/Creatinase_N
dddP homolog	SAR116_0769	metallopeptidase, family M24	Peptidase_M25/Creatinase_N
dddQ	SAR116_0023	Cupin 2 barrel domain-containing protein (EC:2.7.7.22)	Cupin_2/ARD/AraC_binding/Cupin_6/ MannoseP_isomer/AraC_binding_2/Cupin_3
dddQ homolog	SAR116_0050	Cupin 2 conserved barrel domain protein	Cupin_2/AraC_binding/Cupin_1/Cupin_3/CENP-C_C/ARD/AraC_binding_2/HgmA/EutQ
dddW	SAR116_1790	potential Cupin domain-containing protein (EC:5.3.1.9)	Cupin_2/Cupin_1/AraC_binding/MannoseP_isomer GPI/Cupin_6/Auxin_BP
dmdA	SAR116_0074	aminomethyl transferase (EC:2.1.2.10)	GCV_T/GCV_T_C
dmdA homolog	SAR116_0916	glycine cleavage T protein (aminomethyl transferase) (EC:2.1.2.10)	GCV_T/GCV_T_C
dmdA homolog	SAR116_0235	aminomethyltransferase (EC:2.1.2.10)	GCV_T/GCV_T_C/SoxG/TrmE_N
dmdA homolog	SAR116_1344	aminomethyltransferase (glycine cleavage system T protein) (EC:2.1.2.10)	GCV_T/GCV_T_C
dmdA homolog	SAR116_2172	aminomethyl transferase (EC:2.1.2.10)	GCV_T/GCV_T_C

Table 3. Distribution of SAR116 were summarized using published molecular community studies based on 16S rDNA, ARISA*, and CARD-FISH† methods.

Source ID	Isolation Source	Latitude and Longitude	Reference
Marginal Sea	Western Mediterranean Sea	40.67 N 2.87 E	(Acinas SG *et al.*, 1999)
North Atlantic Ocean	400 km South of Iceland	50.00 N 21.0 W	(Gonzalez JM *et al.*, 2000)
Arctic Ocean	Arctic Ocean	75.48 N 145.13 W	(Bano N and Hollibaugh JT, 2002b)
Marginal Sea	Arabian Sea water	20.9 N 63.7 E 3.79 N 67.0 E	(Bernhard MF *et al.*, 2005)
Marginal Sea	California Cooperative Oceanic Fisheries Investigations (CalCOFI) station, 570 km west of Ensenada, Mexico	31.32 N 123.74 W	(Schwalbach M, S. *et al.*, 2005)*
Antarctic Ocean	the Scotia Sea, Antarctica	61.43 S 54.66 W 61.50 S 52.77 W 60.53 S 52.21 W 61.58 S 46.07 W 58.74 S 41.69 W 54.91 S 39.99 W 56.54 S 37.93 W 55.45 S 34.39 W	(Juliette NT *et al.*, 2006) †
Estuary	Whole surface water from Chesapeake Bay	37.12 N 76.12 W	(Kan J *et al.*, 2008)

Marginal Sea	NW Mediterranean Sea	42.52 N 03.18 E	(Lami R *et al.*, 2009)
Estuary	marine surface waters along the Delaware (USA) coast	38.85 N 75.11 W	(Campbell BJ *et al.*, 2009)
Mediterranean Sea	Gulf of Lyons	42.52 N 3.21 E	(Schäfer H *et al.*, 2000)
Marginal Sea	The Gully, a submarine canyon located at continental shelf off Nova Scotia near Sable Island	43.84 N 58.90 W	(Yeung CW *et al.*, 2010)
North Sea	Northern Part of North Sea	60.0 N 3.0 E	(Zubkov MV *et al.*, 2002)
North Pacific Ocean	DNA collected from Monterey Bay, CA	36.78 N 122.48 W	(Béjà O *et al.*, 2000)
North Pacific Ocean	plankton DNA extracts from surface water, Monterey Bay, CA	35.44 S 124.89 W	(Suzuki MT *et al.*, 2001)
Great Barrier Reef, Australia	Coral micobial community, Davies Reef	18.85 S 147.68 E	(Bourne DG and Munn CB, 2005)
San Pedro Ocean Time Series (SPOTS)	bacterioplankton DNA collected at 5M depth	33.55 N 118.40 W	(Brown MV *et al.*, 2005)
North Atlantic Ocean	Surface (- 2 m) & chlorophyll maximum, Gulf Stream Ring	39.7 N 69.85 W	(Lau WWY and Armbrust EV, 2006)
North Eastern Pacific Deep Sea	oceanic crustal fluids; deep-sea water near Baby Bare Seamount, North East Pacific	47.42 N 127.47 W	(Huber JA *et al.*, 2006)
Salt marsh tidal creek	Dean Creek (a salt marsh tidal creek on Sapelo Island, GA)	31.3929 N 81.2699	(Mou X *et al.*, 2007)

Panama Pacific	250 miles from Panama City	6.49 N 82.9 W	
Panama Atlantic	Northeast of Colon, Panama	10.72 N 80.25 W	
North Atlantic Ocean	Chesapeake Bay, MD	38.95 N 76.42 W	(Shaw AK *et al.*, 2008)
North Atlantic Ocean	Delaware Bay, NJ	39.42 N 75.5 W	
North Atlantic Ocean	Newport Harbour, RI	41.49 N 71.35 W	
Southern Indian Ocean	3 micron prefiltered seawater from 100 m depth (station C11), Kerguelen Plateau	51.39 S 78.00 E	(West NJ *et al.*, 2008)
	3 micron prefiltered seawater from 120 m depth (station A3), Kerguelen Plateau	50.38 S 72.05 E	
North Atlantic Ocean	surface water at the UGA Marine Institute	31.4 N 81.28 W	(Poretsky RS *et al.*, 2010)
Coast	Oregon coast study, East Pacific Ocean	44.65 N 124.18 W	(Rappe MS *et al.*, 2000)
Marginal Sea	Porcupine Abyssal Plain (PAP) water column, Eastern North Atlantic	48.83 N 16.5 W	(Gallagher JM *et al.*, 2004)
Coast	Oregon Coast	44.65 N 124.18 W	(Stingl U *et al.*, 2007b)

North eastern New Zealand	Sponge-associated microbial community from Mathesons Bay and Jones Bay,	36.3 S 174.78 E	(Kamke J *et al.*, 2010)
Coral Reef	Paopao Bay, Moorea, French Polynesia	17.48 S 149.82 W	(Nelson CE *et al.*, 2011)
North Atlantic Ocean	Sargasso Sea	32.07 N 64.38 W	(Mullins TD *et al.*, 1995)
North Atlantic Ocean	continental shelf off Cape Hatteras, North Carolina	35.983 N 75.133 W	(Rappé MS *et al.*, 1997)
North Atlantic Ocean	Sargasso Sea	32 N 64 W	(Morris RM *et al.*, 2005)
Marine Sponge	Adriatic Sea, marine sponge associated seawater	45.13 N 13.67 E	(Althoff K *et al.*, 1998)
Coral Reef	Crawl Cay reef near Bocas del Toro, Caribbean Sea	9.15 N 82.117 W	(Sunagawa S *et al.*, 2010)
North Atlantic Ocean	Sargasso Sea waters	31.1585 N 64.010 W 31.0175 N 64.324 W 31.535 N 63.595 W 32.167 N 64.30 W	(Venter JC *et al.*, 2004)
North Eastern Pacific Ocean	Saanich Inlet	48.59 N 123.5 W	(Walsh DA *et al.*, 2009)
Marginal Sea	East Sea of Korea	38.34 N 128.56 E	In this study

Table 4. Clone libraries citing SAR116 were summarized using arb-silvar rel 106.

Collections of 16S rRNA genes from culture independent studies referring SAR116 were added into reference trees in silva using parsimony-method. Clone IDs' were counted for binning into cross-Tables according to latitudes and longitudes of each sample sources.

Source ID	Isolation Source	Latitude and Longitude	Clone ID's	SAR11	RCA	SAR86	SAR116	Other clades	Reference
North Atlantic Ocean	400 km South of Iceland	50.0 N 21.0 W	43	27.9%	30.2%	2.3%	16.3%	23.3%	(Gonzalez JM *et al.*, 2000)
Arctic Ocean	Arctic Ocean	75.48 N 145.13 W	13	23.1%	0.0%	0.0%	7.7%	69.2%	(Bano N and Hollibaugh JT, 2002b)
Arabian Sea	Arabian Sea water	19.0 N 67.0 E	106	22.6%	0.0%	0.0%	1.9%	75.5%	(Bernhard MF *et al.*, 2005)
		20.9 N 63.7 E	106	7.5%	1.9%	1.9%	7.5%	81.1%	
		3.79 N 67.0 E	57	22.8%	0.0%	3.5%	14.0%	59.6%	
North Atlantic Ocean	Whole surface water from Chesapeake Bay	37.12 N 76.12 W	90	12.2%	20.0%	3.3%	4.4%	60.0%	(Kan J *et al.*, 2008)
		38.3 N 76.28 W	98	9.2%	11.2%	0.0%	4.1%	75.5%	
		39.13 N 76.33 W	94	5.3%	25.5%	0.0%	2.1%	67.0%	
Mediterranean Sea	Gulf of Lyons	42.52 N 3.21 E	18	0.0%	16.7%	5.6%	22.2%	55.6%	(Schäfer H *et al.*, 2000)
North Sea	Northern Part of North Sea	60.0 N 3.0 E	18	11.1%	5.6%	5.6%	16.7%	61.1%	(Zubkov MV *et al.*, 2002)

Panama Atlantic	Northeast of Colon, Panama	10.72 N 80.25 W	955	39.4%	4.3%	4.0%	9.7%	42.6%	
North Atlantic Ocean	Chesapeake Bay, MD	38.95 N 76.42 W	1078	38.2%	0.4%	0.2%	0.6%	60.6%	(Shaw AK *et al.*, 2008)
North Atlantic Ocean	Delaware Bay, NJ	39.42 N 75.5 W	1091	36.2%	0.6%	1.4%	1.1%	60.7%	
North Atlantic Ocean	Newport Harbour, RI	41.49 N 71.35 W	1077	11.2%	38.6%	8.3%	9.8%	32.0%	
Panama Pacific	250 miles from Panama City	6.49 N 82.9 W	1352	39.3%	5.1%	4.5%	8.2%	42.9%	
Kerguelen Plateau, Southern Indian Ocean	3 micron prefiltered seawater from 120 m depth (station A3)	50.38 S 72.05 E	188	9.6%	25.5%	0.0%	6.9%	58.0%	(West NJ *et al.*, 2008)
	3 micron prefiltered seawater from 100 m depth (station C11)	51.39 S 78.00 E	146	18.5%	15.8%	2.1%	9.6%	54.1%	
North Atlantic Ocean	surface water at the UGA Marine Institute	31.4 N 81.28 W	511	14.1%	9.2%	3.3%	6.1%	67.3%	(Poretsky RS *et al.*, 2010)
North Pacific Ocean	DNA collected from Monterey Bay, CA	36.78 N 122.48 W	22	13.6%	13.6%	13.6%	9.1%	50.0%	(Béjà O *et al.*, 2000)
North Pacific Ocean	plankton DNA extracts from surface water, Monterey Bay, CA	35.44 S 124.89 W	27	25.9%	3.7%	22.2%	18.5%	29.6%	(Suzuki MT *et al.*, 2001)
Great Barrier Reef, Australia	Coral micobial community, Davies Reef	18.85 S 147.68 E	73	9.6%	2.7%	2.7%	8.2%	76.7%	(Bourne DG and Munn CB, 2005)
San Pedro Ocean Time Series (SPOTS)	bacterioplankton DNA collected at 5M depth	33.55 N 118.40 W	174	23.0%	12.1%	6.9%	6.9%	51.1%	(Brown MV *et al.*, 2005)

	bacterioplankton DNA collected at 500M depth	33.55 N 118.40 W	32	12.5%	0.0%	0.0%	9.4%	78.1%	
North Pacific Ocean	surface water	48.57 N 123.02 W	68	1.5%	14.7%	0.0%	8.8%	75.0%	
North Atlantic Ocean	Gulf Stream Ring surface at 2 m	39.7 N 69.85 W	38	34.2%	2.6%	2.6%	7.9%	52.6%	(Lau WWY and Armbrust EV, 2006)
	Gulf Stream Ring chlorophyll maximum	39.7 N 69.85 W	36	47.2%	5.6%	2.8%	2.8%	41.7%	
North Eastern Pacific Deep Sea	oceanic crustal fluids; deep-sea water near Baby Bare Seamount, North East Pacific	47.42 N 127.47 W	152	2.6%	0.7%	1.3%	1.3%	94.1%	(Huber JA *et al.*, 2006)
North eastern New Zealand	Sponge-associated microbial community from Mathesons Bay and Jones Bay,	36.3 S 174.78 E	313	0.0%	1.6%	26.5%	0.6%	71.2%	(Kamke J *et al.*, 2010)
North Atlantic Ocean	continental shelf off Cape Hatteras, North Carolina	35.983 N 75.133 W	41	2.4%	9.8%	9.8%	4.9%	73.2%	(Rappé MS *et al.*, 1997)
North Atlantic Ocean	Sargasso Sea waters	32 N 64 W	27	14.8%	11.1%	3.7%	11.1%	59.3%	(Morris RM *et al.*, 2005)

Caribbean Sea	Crawl Cay reef near Bocas del Toro	9.15 N 82.117 W	342	13.2%	4.4%	2.9%	2.6%	76.9%	(Sunagawa S *et al.*, 2010)
North Atlantic Ocean	Sargasso Sea waters	31.1585 N 64.010 W 31.175 N 64.324 W 31.535 N 63.595 W 32.167 N 64.30 W	2160	35.3%	3.2%	3.1%	7.8%	50.6%	(Venter JC *et al.*, 2004)
North Eastern Pacific Ocean; Saanich Inlet	10 m depth	48.59 N 123.5 W	1038	14.2%	19.2%	1.6%	5.2%	59.8%	(Walsh DA *et al.*, 2009)
	100 m depth	48.59 N 123.5 W	1199	16.2%	2.6%	0.4%	1.4%	79.4%	
	120 m depth	48.59 N 123.5 W	1308	9.0%	2.4%	0.2%	1.7%	86.6%	
	125 m depth	48.59 N 123.5 W	386	1.6%	0.3%	0.0%	0.3%	97.9%	
	200 m depth	48.59 N 123.5 W	1267	2.6%	0.4%	0.2%	0.2%	96.6%	
Average %				17.0%	8.7%	4.0%	7.0%	63.4%	
Maximum %				47.22 %	38.63 %	26.52 %	22.22 %	97.93 %	

Table 5. Basic Taxonomical Observation of Strain IMCC1322.

Colony morphology was tested on modified R2A agar after 4-week incubation at 25 ℃. Temperature, salinity, and pH profiles were recorded using

Colony Morphology	
color	pale reddish
size	0.05-0.1mm
pigments (by eye)	+
pigments (extraction, spectroscopy)	-
shape	circular, smooth, entire, opaque, convex
gliding motility	-

Gram staining	-

Growth Conditions

optimum medium	Modified R2A prepared in Aged Sea Water
growth temperature	12.8 ~ 34.2 ℃
optimum temp	25.5 ℃
pH range	7.0~7.4
Sodium requirement	+

Table 6. Cellular fatty acid composition of strain IMCC1322.

Monounsaturated fatty acid esters of C16:1 (Summed Feature 3) and C18:1 (Summed Feature 8) were the major fatty acid components for strain IMCC1322 and polyunsaturated fatty acid, C20:4(n-6) was also detected.

Fatty acid	%
$C_{10:0}$ 3OH	1.6
$C_{16:0}$	3.08
$C_{17:0}$ cyclo	0.66
$C_{18:0}$	0.54
$C_{19:0}$	0.86
$C_{20:4}$ ω6,9,12,15c	1.02
Summed Feature 3†	49.78
Summed Feature 6‡	0.86
Summed Feature 7*	1.63
Summed Feature 8§	39.98

†Summed Feature 3 is C16:1 ω7c/C16:1 ω6c

‡Summed Feature 6 is C19:1 ω11c/C19:1 ω9c

*Summed Feature 7 is C19:1 ω6c/ C19:1 ω7c/19cy

§Summed Feature 8 is C18:1 ω7c/C18:1 ω6c

Table 7. Membrane transport system from genome annotation of IMCC1322.

Type/cds	Abbreviations	Comments
General amino acid ABC transporter for His/Glu/Gln/Arg/opine		
SAR116_0332~5 SAR116_0448~52	aapJQMP	General L-amino acid transport
Branched-chain amino acid ABC transporter		
SAR116_1784~8 SAR116_0346~50 SAR116_0928~32 SAR116_1458~61 SAR116_0779~83 SAR116_1756~60	livBFGHKM	high affinity branched-chain amino acid ABC transporter for Leu/Ile/Val
SAR116_1623	livM	periplasmic component
Polar amino acid ABC transporter		
SAR116_0306~9 SAR116_1443~6	ABC.PA.A ABC.PA.P ABC.PA.S	polar amino acid ABC transporter, inner membrane subunit
Proline/glycine betaine transporter		
SAR116_1389~91	proXWV	ABC proline/glycine betaine transporter
SAR116_0452		BCCT transporter
ABC heme exporter		
SAR116_1076~8	ccmABC	Cytochrome c biogenesis ATP-binding export protein ccmABC
ABC metal transporter		
SAR116_0772	ABC.FE.P	ABC-type Fe^{3+} transport system, permease component.
SAR116_0020		ABC-type transport system involved in Fe-S cluster assembly, permease and ATPase components
SAR116_2225~7		high-affinity zinc uptake system abc transporter
N/P/S compound transporters		
SAR116_2099~101	msmEFG	Putative ABC MSA transporter
SAR116_2095 SAR116_2097~8	nrtABC	nitrate ABC transporter
SAR116_0080	phnE	phosphonate ABC permease

SAR116_1206~2	pstSCAB	phosphate ABC transporter
SAR116_0590~2	ABC.TG.P ABC.TG.S ABC.TG.A	sulfate/tungstate uptake family ABC transporter
SAR116_1439~41	tauABC	sulfonate/nitrate/taurine transport
Organic solvent resistance ABC transporter		
SAR116_0647~8 SAR116_2533~4	ABC.X1.P/ABC.X1.A ABC.X1.P/ABC.X2.A	ABC-type transport system involved in resistance to organic solvents
Oligopeptide/dipeptide ABC transporter		
SAR116_0064~7 SAR116_0948~52 SAR116_1524~8	ABC.PE.S ABC.PE.P ABC.PE.A	oligopeptide/dipeptide ABC transporter
Polyamine ABC transporter		
SAR116_0758~61 SAR116_1721~4 SAR116_1791~4 SAR116_2031~3	potABCD	Spermidine/putrescine ABC transporter
Sugar ABC transporter		
SAR116_1769~71	rbsABC	Ribose/xylose/arabinose/galactoside ABC-type transport systems
SAR116_0967~70	smoEFGK	ABC sorbitol/mannitol transporter
SAR116_0042~4 SAR116_0269~71 SAR116_0886~90 SAR116_1197~9 SAR116_1606~9	msmEFG	sugar ABC transporter
SAR116_1192	thuK	ABC transporter, nucleotide binding/ATPase protein [trehalose/maltose]
SAR116_2316	xylG	putative D-xylose transport ATP-binding protein xylG
Lipoprotein releasing ABC transporter		
SAR116_0521~2	lolD/lolCE	Lipoprotein-releasing system ATP-binding protein lolD 1 (EC 3.6.3.-).
Other ABC transporters		
SAR116_2053	ATPase	Putative ABC transporter, fused ATPase subunits.

SAR116_1880	Permase	Predicted ABC-type multidrug transport system permease component.
SAR116_2094	gldG	ABC-type uncharacterized transport system involved in gliding motility auxiliary component-like protein
SAR116_2258	natA	ABC-type transport protein slr1901
Unknown ABC transporter proteins		
SAR116_0959~61		ATP-binding protein
SAR116_1967		ABC transporter
SAR116_0600~2		putative ABC transporter
SAR116_0894~6		ABC-2
SAR116_0909		Putative permease
SAR116_1418 SAR116_2318		ABC transporter component
SAR116_0416 SAR116_1130 SAR116_1270 SAR116_2347 SAR116_2520 SAR116_1510~2		ABC transporter related
SAR116_1954 SAR116_2069		ABC transporter, transmembrane region
SAR116_2279		ATP-binding/permease protein, ABC transporter, membrane spanning protein
SAR116_1342		Abc1 protein
SAR116_0608 SAR116_0911 SAR116_1247 SAR116_1309		putative ATP-binding protein
SAR116_2466~9		ABC transporter
Volatage gated Chloride channel		
SAR116_0838	clc	Cl^- channel, voltage-gated family protein
Antiporter		
SAR116_0463~7	MnhB/A/G	Na^+/H^+ antiporter MnhB subunit-related protein

SAR116_0219	trkA	K^+ transport systems, NAD-binding component
Symporter		
SAR116_0756		sodium/alanine symporter
SAR116_0788	ssf	Na^+/solute symporter (Ssf family)
SAR116_1515	-	sodium:neurotransmitter symporter family protein
SAR116_1094	-	Chromate transporter
Cation transporter		
SAR116_2475		Divalent cation transporter
SAR116_1886	trkA	Predicted Trk-type K^+ transport system membrane component.
SAR116_0808		Kef-type K^+ transport systems (NAD-binding component)
Efflux system		
SAR116_1162 SAR116_2450		Auxin Efflux Carrier
SAR116_0999 SAR116_0396		Cation efflux protein
SAR116_0567	KefA	Potassium efflux system protein
SAR116_2009		Cation/multidrug efflux pump
SAR116_2481	MATE	MATE(multidrug and toxic compound extrusion) efflux family protein
SAR116_0351 SAR116_1695	MFP	efflux transporter, RND family, MFP subunit
SAR116_0222 SAR116_2243	rht	threonine efflux protein
SAR116_0428		outer membrane efflux family protein
Exporter		
SAR116_0901 SAR116_1181 SAR116_2237~8 SAR116_2493~4	lysE	Lysine exporter protein (LYSE/YGGA)
SAR116_0292	rnd	exporter of the RND superfamily
MFS		

SAR116_0736 SAR116_0021 SAR116_1327 SAR116_2538 SAR116_1754		major facilitator family transporter
Other branched-chain amino acid transporter		
SAR116_0735		branched-chain amino acid transport
Drug resistance transporter		
SAR116_2000	Bcr/CflA	drug resistance transporter, Bcr/CflA subfamily
Metal iron transporter		
SAR116_2091~2		Putative iron binding and permease
SAR116_2222		high-affinity nickel-transporter
Oligoketide cyclase/lipid transport protein		
SAR116_0210		Oligoketide cyclase/lipid transport protein
N/P/S transporters		
SAR116_2108	sulP	Putative sulfate transporter.
SAR116_0933	NARK, narU, nasA	putative major facilitator family (MFS) nitrate transporter
SAR116_0035 SAR116_2434 SAR116_2465	amt	ammonium transporters
Sugar transporters		
SAR116_2137		mannitol transporter
SAR116_0941		sugar (and other) transporter
Nucleotide base transport		
SAR116_1372		xanthine/uracil permease, putative
Other putative transporter proteins		
SAR116_0260 SAR116_2175 SAR116_0479	rarD rhaT	possible transporter, RarD/RhaT family, DMT superfamily

SAR116_1626		Transport-associated precursor.
SAR116_1408 SAR116_1466 SAR116_1617		putative transport transmembrane protein
SAR116_0593		integral membrane transport protein
PTS system for Trehalose		
SAR116_0700		PTS system, trehalose-specific IIBC subunit
SAR116_0705		putative transport protein,
TRAP transporters		
SAR116_0248~50 SAR116_1369~71	DctQMP	C4-dicarboxylate transport system
SAR116_2060~2	DctPQM	TRAP transporter for mannitol/chloroaromatic compounds
SAR116_0480 SAR116_0482	DctP/M	TRAP dicarboxylate transporter-DctP/DctM subunit
SAR116_0057~9 SAR116_0110~2	DctPQM	TRAP dicarboxylate transporter
Type I secretion		
SAR116_2299 SAR116_2297 SAR116_1169	tolB/tolR/tolC	Type I secretion outer membrane protein, TolB/R/C family
SAR116_0813	tolQ	MotA/TolQ/ExbB proton channel
SAR116_1167 SAR116_2008	hlyD	type I secretion membrane fusion protein, HlyD family
SAR116_1655 SAR116_2266		Outer membrane protein (Porin).
Type II Secretion System		
SAR116_2517~18 SAR116_2521 SAR116_2523 SAR116_2526	pilCBMQT	Type II Secretion System

Table 8. Genes encoding regulatory proteins of IMSNU1322.

Type/ORF ID	Abbreviation	Comments
Antibiotic resistance		
SAR116_2205	marR	Transcriptional regulator, MarR family.
SAR116_0291	tetR/acrR	putative regulator (TetR/AcrR family)
SAR116_0836 SAR116_2201	tetR	Transcriptional regulator, TetR family
SAR116_2145		Negative regulator of beta-lactamase expression
Methyl-accepting chemotaxis related signal transducer		
SAR116_0194		Methyl-accepting chemotaxis protein
SAR116_0816 SAR116_0856		methyl-accepting chemotaxis sensory transducer
SAR116_1281		methyl-accepting chemotaxis transducer
SOS response		
SAR116_0502	lexA	LexA repressor
SAR116_0162	nrdR	Transcriptional repressor nrdR.
Metalloregulators		
SAR116_2180	arsR	ArsR family Transcriptional Regulator
SAR116_1155 SAR116_1571 SAR116_2224	fur	Fur family transcriptional regulator
SAR116_0174	merR	MerR family Transcriptional Regulator
SAR116_1403		Iron dependent repressor
SAR116_1110		putative suppressor for copper-sensitivity B precursor
Nitrogen metabolism		
SAR116_0216 SAR116_0218	fis-type	Nitrogen regulation protein NR(I)
SAR116_0107	glnB	Nitrogen regulatory protein P-II
SAR116_2464	glnK	nitrogen regulatory protein P-II 2

SAR116_0215 SAR116_0217	ntrB	Signal transduction histidine kinase involved in nitrogen fixation and metabolism regulation
SAR116_1248		probable nitrogen regulatory IIA protein
Phosphorus uptake		
SAR116_1201	phoB	two component transcriptional regulator, winged helix family
SAR116_1207	phoR	Periplasmic Sensor Signal Transduction Histidine Kinase precursor
SAR116_1589	phoH	Putative phosphate starvation-induced protein
SAR116_1993	ppx	Ppx/GppA phosphatase for modulation of ppGpp
Sigma factor related		
SAR116_0834~5	fis	σ^{54} specific transcriptional regulator, fis family
SAR116_0857	flgM	putative anti-σ^{28} factor, FlgM
SAR116_0865	σ^{28},fliA/whiG	RNA polymerase, σ^{28} subunit, FliA/WhiG
SAR116_1643	rho	Transcription termination factor
SAR116_2233 SAR116_2470	σ^{70},rpoD	σ^{70} (RpoD)
SAR116_2314	σ^{32},rpoH	RNA polymerase, σ^{32} subunit, RpoH
SAR116_2528	spoIIAA	Anti-anti-sigma regulatory factor
Stress related genes		
SAR116_1407 SAR116_2174	csp	cold shock protein
SAR116_0086 SAR116_1188	DksA	DnaK suppressor protein
SAR116_1356 SAR116_1908	DnaJ	heat shock protein DnaJ domain protein
SAR116_0757 SAR116_2177 SAR116_0119	usp	universal stress protein family protein
SAR116_1619		Negative regulator of class I heat shock protein
SAR116_1582	nusA	NusA antitermination factor
SAR116_0167	nusB	NusB antitermination factor

SAR116_1951 SAR116_2379	nusG	Transcription antiterminator
GntR family		
SAR116_0245 SAR116_0054 SAR116_0310 SAR116_0323 SAR116_1743 SAR116_2024	gntR	Transcriptional regulator, GntR family protein.
LacI family		
SAR116_0971 SAR116_0048 SAR116_0917	lacI	LacI family transcriptional regulator
Lambda repressor-like transcription regulator		
SAR116_1467		helix-turn-helix domain protein
SAR116_1898		transcriptional regulator
Other transcriptional regulator		
SAR116_0239 SAR116_1200 SAR116_1398 SAR116_2125 SAR116_2160 SAR116_2236	araC	AraC family transcriptional regulator
SAR116_1950 SAR116_2220 SAR116_2541	asnC	AsnC family Transcriptional Regulator
SAR116_0897	badM/rrf2	BadM/Rrf2 family transcriptional regulator
SAR116_0227 SAR116_1070	carD	Transcription factor CarD
SAR116_1658 SAR116_2204	cheY	CheY-like Transcriptional regulatory protein
SAR116_0606 SAR116_2067	crp/fnr	Crp/Fnr family transcriptional regulator
SAR116_2228	greA/B	Transcription elongation factor

SAR116_2287	htA	Transducer HtA protein.
SAR116_0297 SAR116_2133	iclR	IclR family transcriptional regulator
SAR116_0070 SAR116_0257 SAR116_0336 SAR116_0934 SAR116_1530 SAR116_1768 SAR116_2052 SAR116_2110 SAR116_2116 SAR116_2372 SAR116_2463	lysR	LysR family transcriptional regulator
SAR116_1083	metR	transcriptional regulator MetR
SAR116_0620 SAR116_1513	rok	ROK family transcriptional regulator,
SAR116_0108	rpiR	transcription regulator, RpiR family, putative
SAR116_1969	tenA	transcriptional activator, TenA family
SAR116_1970	tenA/thi4	TENA/THI-4 family protein
SAR116_1215 SAR116_1631 SAR116_2474	xre	Transcriptional Regulator, XRE family
SAR116_1939		transcriptional coactivator/pterin dehydratase

Unclassifed two component system proteins

SAR116_2181 SAR116_2441	multi-sensor hybrid histidine kinase
SAR116_2530	multi-sensor signal transduction histidine kinase
SAR116_1207 SAR116_2082 SAR116_2203	periplasmic sensor signal transduction histidine kinase
SAR116_1553~4	periplasmic sensor signal transduction histidine kinase & response regulator
SAR116_2257	putative redox sensing protein

SAR116_2359	LytTr/AlgR	Response regulator of the LytR/AlgR family
SAR116_1736		response regulator protein
SAR116_1266~7		histidine kinase & transcriptional regulator
SAR116_1504		hybrid sensor and regulator
SAR116_0085		transcriptional regulator
Unclassified regulators		
SAR116_1763 SAR116_1877	luxR	LuxR family transcriptional regulator
SAR116_0490		Negative transcriptional regulator
SAR116_0418 SAR116_1068		Predicted transcriptional regulator
SAR116_0879		dual specificity protein phosphatase
SAR116_0156 SAR116_0914 SAR116_1395		putative transcriptional regulator protein
SAR116_1602		SH3, type 3 domain protein
SAR116_0127		transcriptional regulator
SAR116_0363		transcription-repair coupling factor
SAR116_0738		transcriptional coactivator/pterin dehydratase
SAR116_0882		transcriptional regulator, putative
SAR116_0957		transcriptonal regulator
SAR116_1287		Uncharacterized coiled-coil protein with Tetratricopeptide repeat domain protein
SAR116_1333		Uncharacterized conserved small protein containing a coiled-coil domain

Table 9. Relative distribution of ORF's annotated as ABC-type and ATP-independent membrane transporters among genomes harboring opsin and related genes.

Genome sizes were divided by the smallest genomic length from "Methylophilales bacterium HTCC2181" (ZP_01551538) and relative genome sizes are given in percentage values. Each ORF's were also divided by the value from HTCC2181 (ZP_01551538)

Organism	Accessions	Description for Opsin	Genome size (bp)	Rel. Genome size (%)	ABC transporters (%)	Antiporters (%)	Symporters(%)	TRAP (%)	Etc (%)	Sum of Transporters (%)	Sum of Transporters (%)/genome(%) [rank]
Methylophilales bacterium HTCC2181	ZP_01551538	hypothetical protein MB2181_00945 (YP)	1304428	100	91	2.2	6.7	0.0	0.0	100	100 [20]
Candidatus Pelagibacter ubique HTCC1062	YP_266049	Proteorhodopsin	1308759	100	140	2.2	6.7	20.0	6.7	178	177.2 [7]
Candidatus Pelagibacter ubique HTCC1002	ZP_01264205	Proteorhodopsin	1327604	102	140	4.4	6.7	17.8	0.0	169	165.9 [11]
Halobacterium sp. NRC-1	NP_280508/ NP_280292/ NP_280434	Sop2/Bop/Sop1	2014239	154	96	26.7	0.0	0.0	35.6	158	102.2 [19]
Natronomonas pharaonis DSM 2160	YP_331142	Sensory rhodopsin II	2595221	199	236	31.1	4.4	8.9	11.1	291	146.3 [16]
Gammaproteobacterium HTCC2207	ZP_01223638	Bacteriorhodopsin	2620870	201	127	8.9	28.9	6.7	4.4	176	87.4 [23]
Polaribacter irgensii 23-P	ZP_01117885	Bacteriorhodopsin	2745458	210	118	11.1	24.4	0.0	4.4	158	75 [27]
Strain IMCC1322	CP001751	Proteorhodopsin	2753527	211	402	11.1	6.7	37.8	113.3	571	270.6 [1]
Flavobacteria bacterium BAL38	ZP_01734914	Bacteriorhodopsin	2806989	215	151	13.3	24.4	2.2	4.4	196	90.9 [22]

Halorubrum lacusprofundi ATCC 49239	ZP_02016140	Rhodopsin	2824790	217	247	48.9	15.6	11.1	20.0	376	173.4 [9]
Polaribacter dokdonensis MED152	ZP_01054176	Bacteriorhodopsin	2967100	227	120	11.1	22.2	0.0	6.7	160	70.3 [29]
Exiguobacterium sibiricum 255-15	ZP_00537900	Rhodopsin	3030158	232	198	24.4	26.7	0.0	37.8	369	158.8 [12]
Haloquadratum walsbyi DSM 16790	YP_656801/ YP_656804	Bacteriorhodopsin precursor (Squarebop I & II)	3132494	240	307	35.6	8.9	11.1	6.7	369	153.6 [14]
Rubrobacter xylanophilus DSM 9941	YP_644794	Rhodopsin	3225748	247	322	28.9	17.8	2.2	6.7	433	175.2 [8]
Dokdonia donghaensis MED134	ZP_01049273	Bacteriorhodopsin	3301953	253	158	13.3	26.7	0.0	2.2	200	79 [25]
Haloarcula marismortui ATCC 43049	YP_135281/ YP_134805/ YP_136594 YP_137573	Opsin of unknown function/sensory rhodopsin 1 /bacteriorhodopsin precursor/bacteriorhodopsin	3419774	262	373	42.2	17.8	2.2	44.4	484	184.8 [5]
Salinibacter ruber DSM 13855	YP_445623/ YP_446872	Xanthorhodopsin (XR)/Halorhodopsin (HR)	3551823	272	144	20.0	22.2	4.4	33.3	233	85.7 [24]
Fulvimarina pelagi HTCC2506	ZP_01440547	Hypothetical protein FP2506_02250	3802689	292	516	35.6	22.2	86.7	0.0	660	226.4 [3]
Marine gammaproteobacterium HTCC2143	ZP_01616930	Bacteriorhodopsin	3925629	301	213	13.3	46.7	17.8	2.2	293	97.5 [21]
Gloeobacter violaceus PCC 7421	NP_923144	Similar to bacterioopsin	4659019	357	238	6.7	0.0	0.0	22.2	273	76.5 [26]
Kineococcus radiotolerans SRS30216	YP_001361545	Rhodopsin	4761183	365	404	31.1	13.3	8.9	11.1	649	177.8 [6]

Rhodobacterales bacterium HTCC2255	ZP_01447408/ZP_01449284	Bacteriorhodopsin	4812704	369	458	51.1	26.7	95.6	31.1	682	184.9 [4]
Marinobacter sp. ELB17	ZP_01737880	Hypothetical protein MELB17_06684	4894744	375	602	53.3	28.9	182.2	4.4	871	232.1 [2]
Photobacterium sp. SKA34	ZP_01161099	Bacteriorhodopsin	4946988	379	480	51.1	46.7	11.1	4.4	596	157 [13]
Vibrio angustum S14	ZP_01236264	Bacteriorhodopsin	5101447	391	487	51.1	40.0	11.1	8.9	598	152.9 [15]
Roseiflexus sp. RS-1	YP_001277280	Rhodopsin	5801598	445	287	15.6	8.9	13.3	17.8	507	113.9 [18]
Vibrio harveyi ATCC BAA-1116	YP_001445352	Hypothetical protein VIBHAR_02160	5969369	458	507	26.7	35.6	35.6	2.2	607	132.6 [17]
Psychroflexus torquis ATCC 700755	ZP_01255583/ZP_01253360	Bacteriorhodopsin	6014448	461	253	31.1	37.8	0.0	4.4	327	70.8 [28]
Methylobacterium sp. 4-46	ZP_01846529	Rhodopsin	7925838	608	793	31.1	46.7	46.7	24.4	1038	170.8 [10]

Table 10. Selected sole carbon source tests for strain IMCC1322.

Positive signs in parenthesis represent weakly positive cultural responses; Turbidity of basal culture medium was recorded in two weeks after IMCC1322 was inoculated. All substrates tested were in 100 μM concentrations and modified R2A in Aged Sea Water was used as basal medium.

Carbon Source Category		Name	Molecular Formula	Growth
Sugar	Monosaccharide	*DL*-glyceraldehyde	$C_3H_6O_3$	+
		D-xylose	$C_5H_{10}O_5$	+
		L-rhamnose	$C_6H_{12}O_5$	(+)
		D-fructose	$C_6H_{12}O_6$	(+)
		D-galactose	$C_6H_{12}O_6$	(+)
		dextrose	$C_6H_{12}O_6$	(+)
		D-mannose	$C_6H_{12}O_6$	(+)
		D-glucosamine hydrochloride	$C_6H_{13}NO_5 \cdot HCl$	-
		sodium gluconate	$C_6H_{11}O_7Na$	+
		D-glucuronic acid sodium salt monohydrate	$C_6H_9O_7Na \cdot H_2O$	(+)
	Disaccharide	*D*-cellobiose	$C_{12}H_{22}O_{11}$	+

		melibiose	$C_{12}H_{22}O_{11}$	+
		D-maltose monohydrate	$C_{12}H_{22}O_{11}\cdot H_2O$	+
		D-lactose monohydrate	$C_{12}H_{22}O_{11}\cdot H_2O$	-
		D-Trehalose	$C_{12}H_{22}O_{11}\cdot 2H_2O$	-
	Trisaccharide	*D*-melezitose	$C_{18}H_{32}O_{16}$	+
		D-raffinose pentahydrate	$C_{18}H_{32}O_{16}\cdot 5H_2O$	(+)
Alcohols	**Sugar alcohol**	meso-erythritol	$C_4H_{10}O_4$	(+)
		adonitol	$C_5H_{12}O_5$	+
		L-arabitol	$C_5H_{12}O_5$	+
		xylitol	$C_5H_{12}O_5$	+
		myo-inositol	$C_6H_{12}O_6$	(+)
		D-mannitol	$C_6H_{14}O_6$	+
		D-sorbitol	$C_6H_{14}O_6$	+
	Alcohol	ethylene glycol	$C_2H_6O_2$	(+)

		glycerol	$C_3H_8O_3$	+
C_1 compound		methanol	CH_4O	+
	Carboxylic acid	formic acid	CH_2O_2	+
	Alkylsulfonic acid	methanesulfonic acid sodium salt	$CH_3O_3S{\cdot}Na$	(+)
Organosulfur compound	**S-containing amino acid**	2-aminoethanesulfonic acid (taurine)	$C_2H_7NO_3S$	(+)
		DL-methionine	$C_5H_{11}NO_2S$	+
		DL-methionine methylsulfonium chloride	$C_6H_{14}NO_2S{\cdot}Cl$	+
	Tertiary Sulfonium	dimethylpropiothetin (DMSP)	$C_5H_{11}O_2S{\cdot}Cl$	+
	Sulfoxide	Dimethylsulfoxide (DMSO)	C_2H_6OS	(+)
Amine	**Tertiary amine**	*N,N*-dimethylglycine	$C_4H_9NO_2$	+
		trimethylamine	C_3H_9N	(+)
	Quaternary amine	betaine hydrochloride	$C_5H_{11}NO_2{\cdot}HCl$	+
		choline chloride	$C_5H_{14}NO{\cdot}Cl$	+
	Quaternary amine /β-Hydroxy acid	*DL*-carnitine hydrochloride	$C_7H_{15}NO_3 \cdot HCl$	(+)
Organic acid	**β-Hydroxy acid**	sodium salicylate	$C_7H_5O_3{\cdot}Na$	(+)
	Acetic acid	potassium acetate	$C_2H_3O_2{\cdot}K$	+

	2-Oxo acid	sodium pyruvate	$C_3H_3O_3 \cdot Na$	(+)
		2,6-diaminopimelic acid	$C_7H_{14}N_2O_4$	(+)
		pimelic acid	$C_7H_{12}O_4$	+
		malonic acid	$C_3H_4O_4$	+
	Dicarboxylic acid	fumaric acid	$C_4H_4O_4$	-
		succinic acid	$C_4H_6O_4$	(+)
		glutaric acid	$C_5H_8O_4$	(+)
		adipic acid	$C_6H_{10}O_4$	(+)
	Tricaboxylic acid	sodium citrate (trisodium salt)	$C_6H_9O_9 \cdot Na_3$	+
	Acetic acid amide	acetamide	C_2H_5NO	+
Amino acid	**Acidic amino acid**	*DL*-glutamine	$C_5H_{10}N_2O_3$	+
		DL-aspartic acid	$C_4H_7NO_4$	+
		L-glutamic acid monosodium salt hydrate	$C_5H_9NO_4$	(+)
	Basic amino acid	*L*-histidine	$C_6H_9N_3O_2$	+
		L-ornithine monohydrochloride	$C_5H_{12}N_2O_2 \cdot HCl$	(+)

	L-arginine monohydrochloride	$C_6H_{14}N_4O_2 \cdot HCl$	+
	DL-lysine dihydrochloride	$C_6H_{14}N_2O_2 \cdot 2HCl$	+
	glycine	$C_2H_5NO_2$	+
Aliphatic amino acid	DL-alanine	$C_3H_7NO_2$	+
	L-leucine	$C_6H_{13}NO_2$	+
Imino acid	*DL*-proline	$C_5H_9NO_2$	(+)
	DL-serine	$C_3H_7NO_3$	(+)
Oxy amino acid	*DL*-threonine	$C_4H_9NO_3$	+

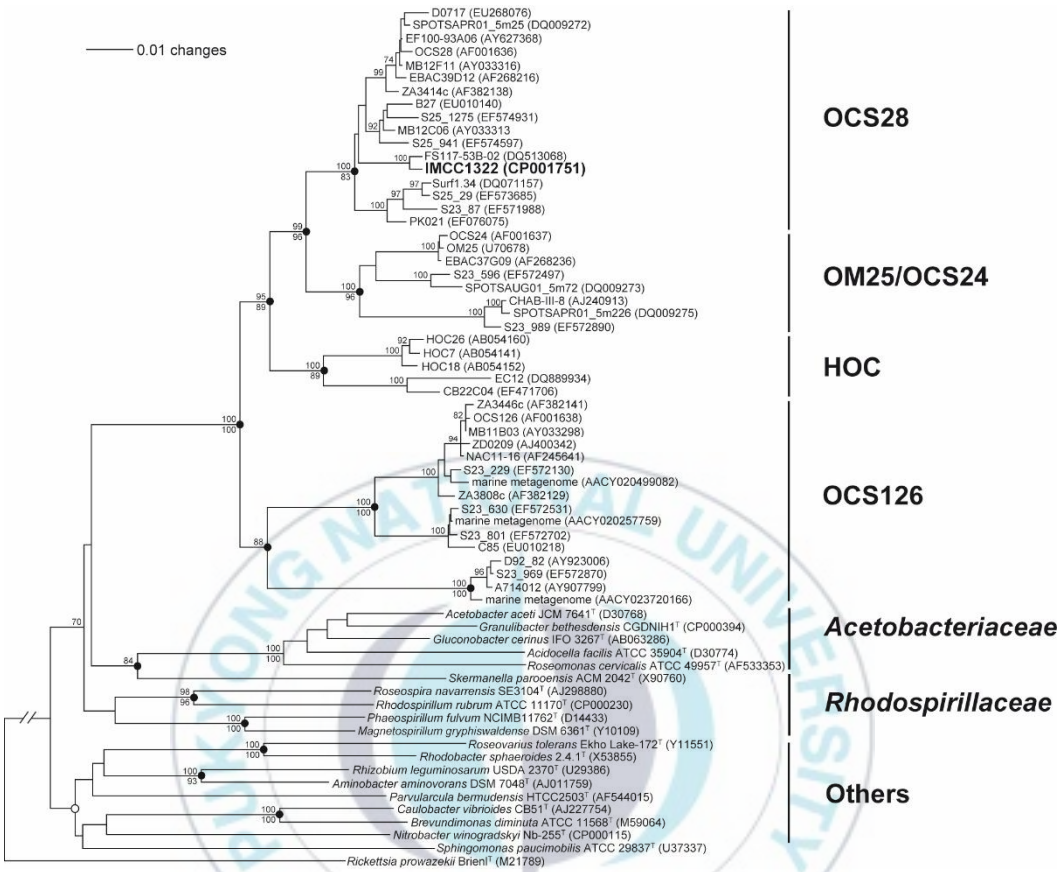

Fig. 1. Phylogenetic relationship of IMCC1322 based on 16S rDNA sequences from 66 taxa.

Sequences include 16S rDNA from uncultured clones and cultured Alphaproteobacteria. Phylogenetic tree were obtained by Neighbour-Joining and Maximum Parsimony methods using Paup4.0b with bootstrap values of 1000 and 100 replicates respectively. Neighbour-Joining tree was drawn with Kimura 2-Parameter whose distance measurement was using 1167 nucleotides (298 characters are excluded from 1465 base-long 16S rRNA alignments). Bootstrap values for NJ/MP were displayed and dots were used to represent nodes that were retained for both of the treeing methods.

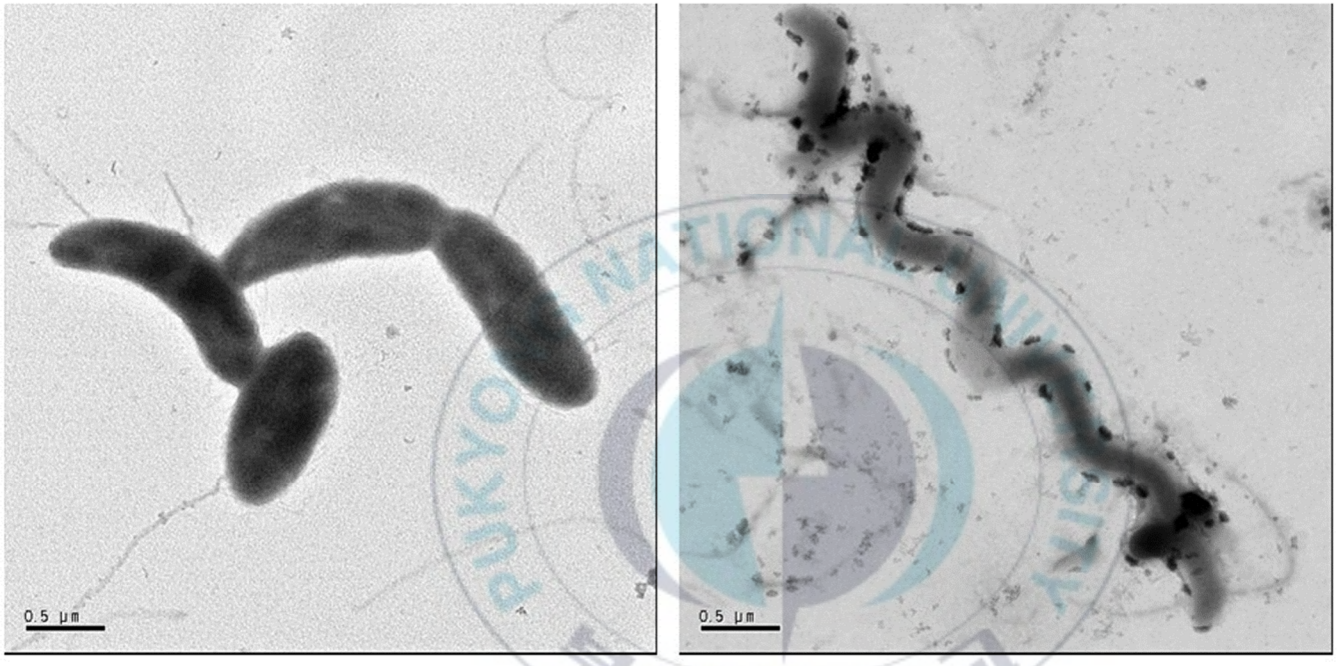

Fig. 2. Transmission electron microscopy (TEM) images of IMCC1322.

Cells grown in 1/10xmPYC liquid were showing the typical vibrioid forms (A).

Early exponential-phase cells exposed to mitomycin C (0.5 μg/ml/ml) overnight (B).

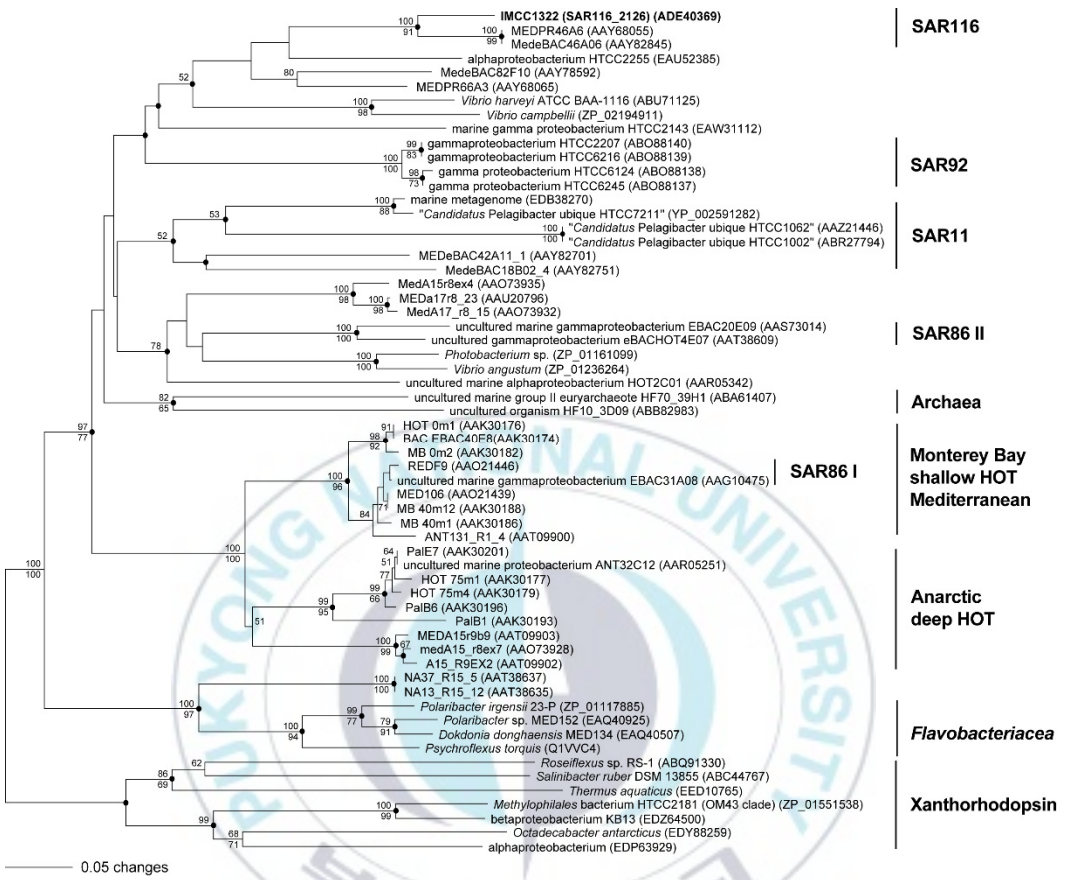

Fig. 3. Phylogeny of proteorhodopsin from IMCC1322 and other proteorhodopsin sequences.

Selected sequences and alignment information were based on PF01036 alignment and phylogenetic tree were obtained by Neighbour-Joining and Maximum Parsimony methods using Paup4.0b with bootstrap values of 1000 and 100 replicates respectively. Included characters for were 134 in number and xanthorhodopsins were used as outgroup. Bootstrap values for NJ/MP were displayed and dots were used to represent nodes that were retained for both of the treeing methods.

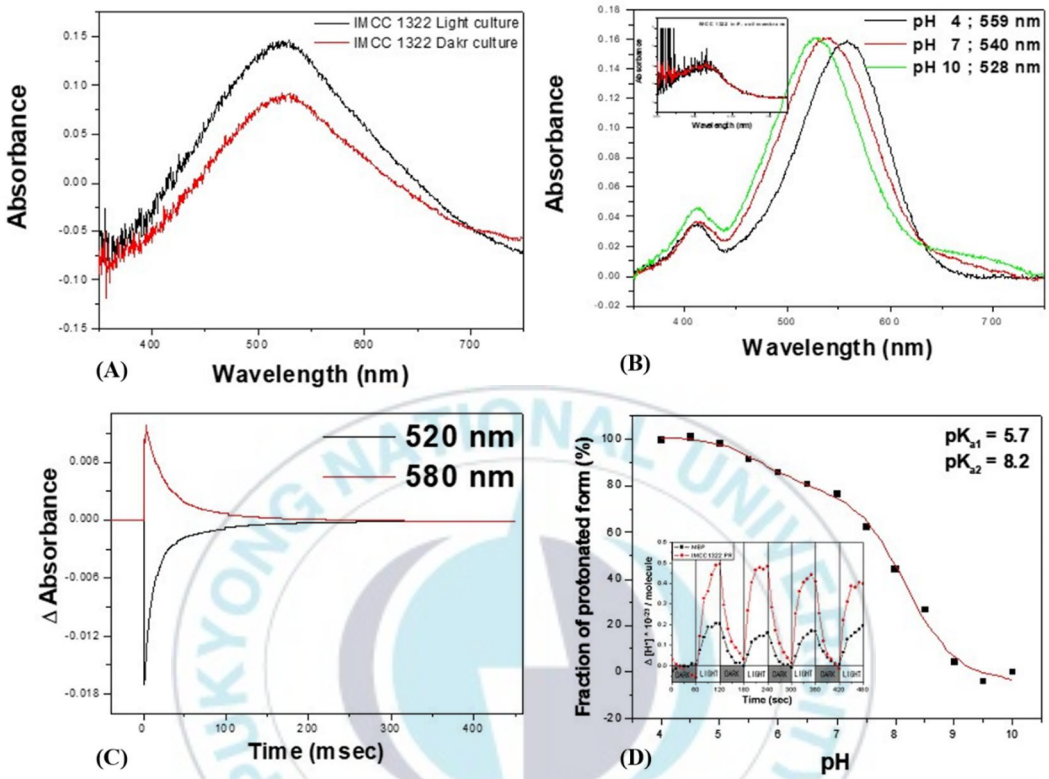

Fig. 4. Spectroscopic assessments of proteorhodopsin from IMCC1322.

(A) Absorption spectrum of IMCC1322 that was cultured in dark condition and light condition shows that it has 522 nm light absorbing pigment. (B) Absorption spectra of purified proteorhodopsins from IMCC1322 at different pH. The absorption maxima at pH 4, 7, and 10 are 559 nm, 519 nm, and 519 nm, respectively. (C) Light-induced absorption difference spectrum of IMCC1322 membrane. (D) Photocycle measurements of IMCC1322 proteorhodopsin in polyacrylamide gel encased membranes at room temperature. After 532-nm flash beam at time 0, the fast creation and decay of photointermediates was monitored at 500 nm, and 600 nm.

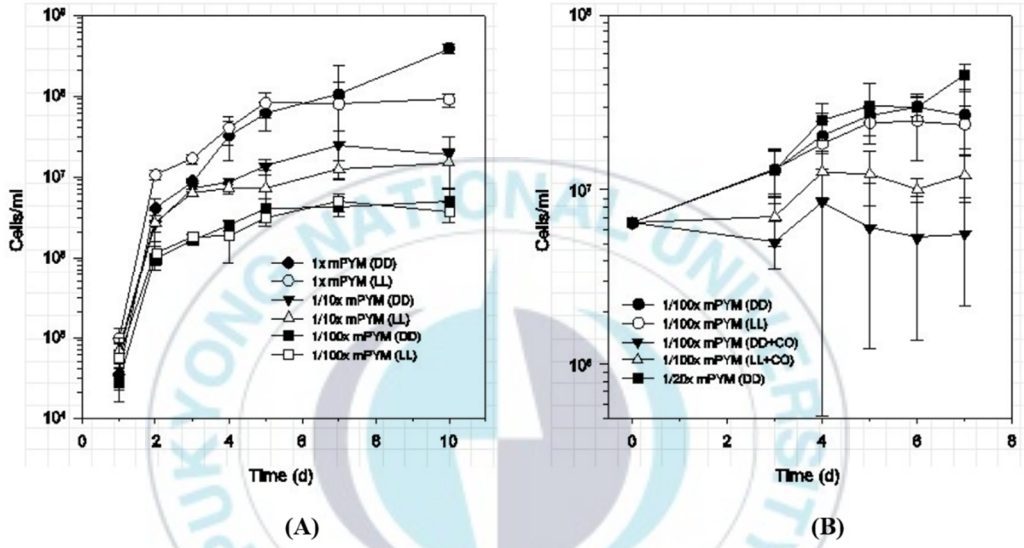

Fig. 5. Comparison of growth responses of IMCC1322 using nutrient level, light, and carbon monoxide (CO).

Cultures were kept under light in 50 ml serum bottles with rubber septum (A) and 50 ml serum bottle with 20% CO in the headspace (B). All data points are triplicated (n=3).

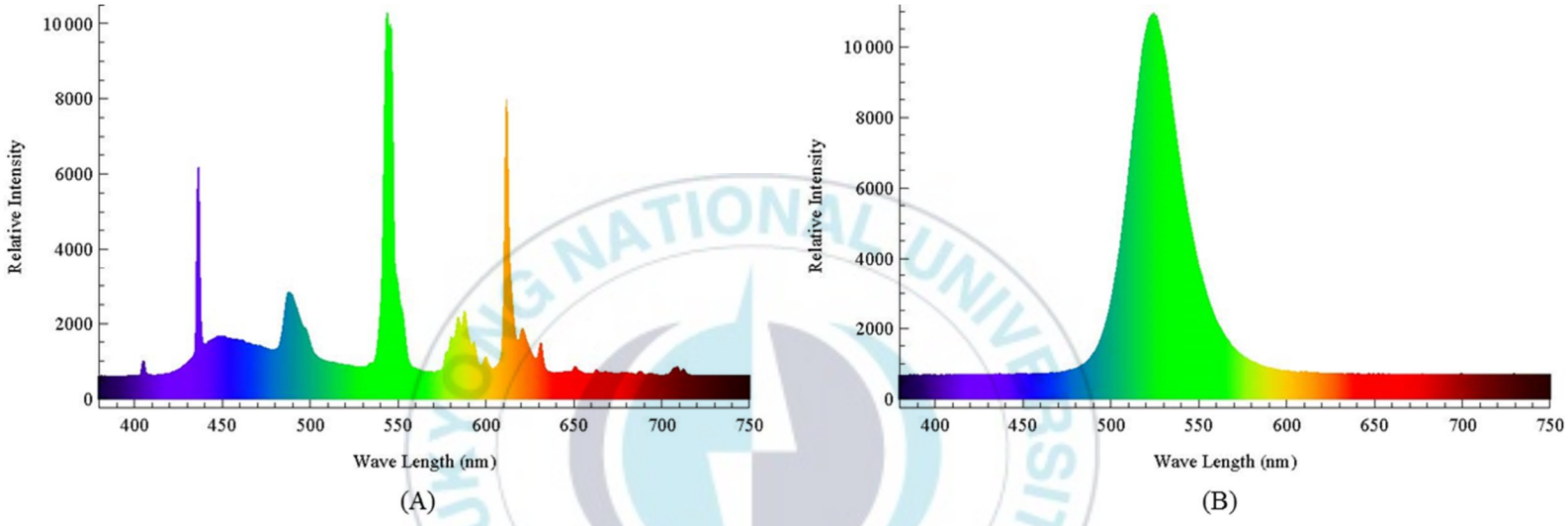

Fig. 6. Wavelength spectra from illumination sources.

Fiber-optic spectrophotometer collected spectra from CFL (A) and LED (B). Monochromatic LED had a peak wavelength at 525.5 nm (B) whereas CFL had no effective emissions around absorption peak by PR of IMCC1322 (522 nm).

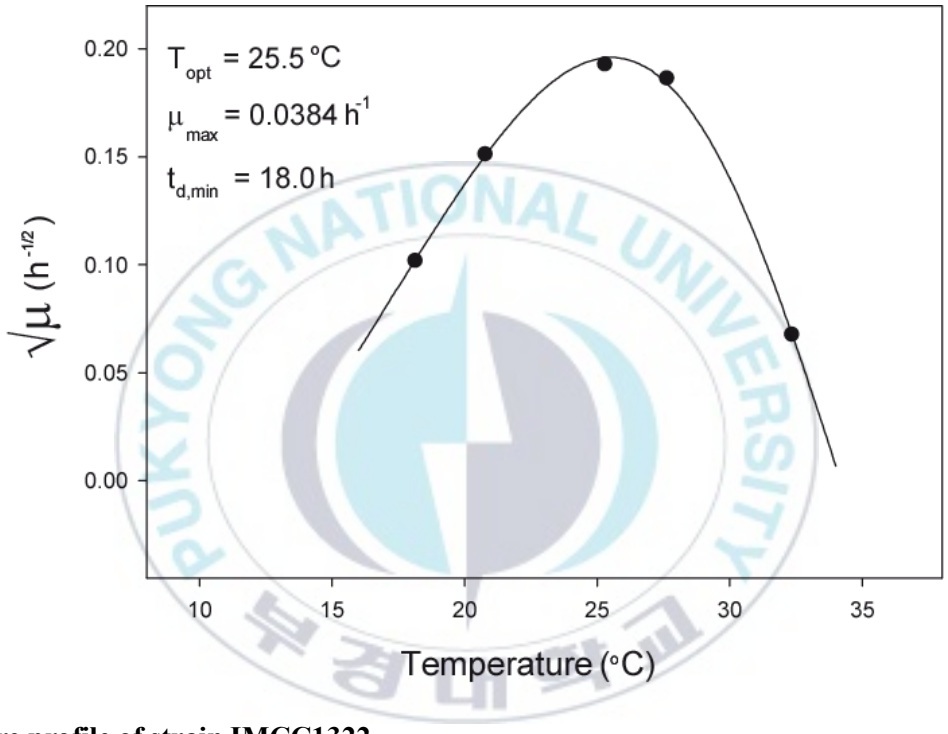

Fig. 7. Growth temperature profile of strain IMCC1322.
The optimal growth temperature of IMCC1322 is 25.5 °C, with the doubling culture time of 18.0 h. OD measurements at 650 nm were recorded using a temperature gradient incubator (TVS-126MA, Advantech Toyo, Japan).

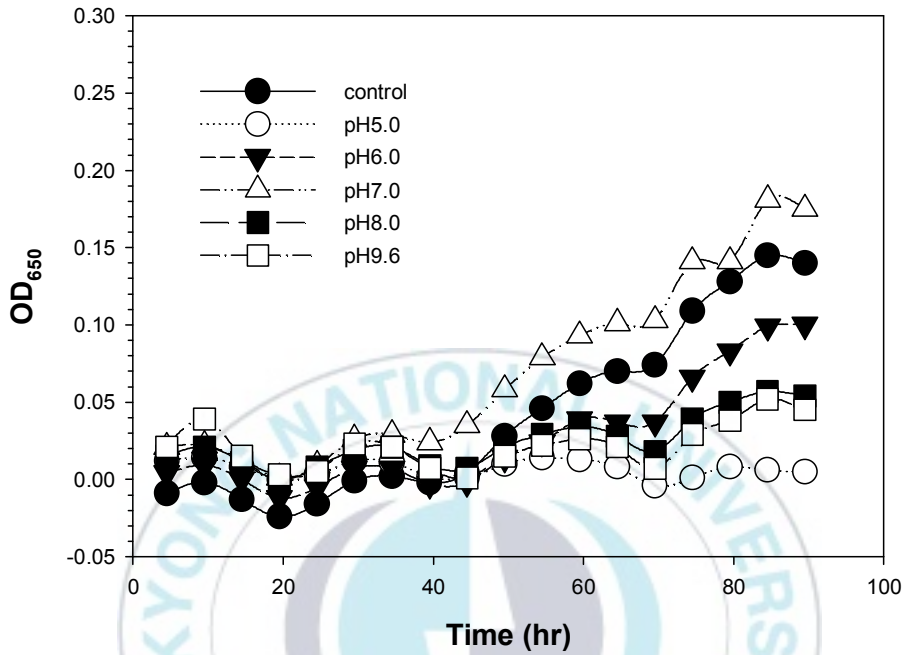

Fig. 8. Salinity range of strain IMCC1322.

The strain was cultured at 25 ℃. OD measurements at 650 nm were recorded using a temperature gradient incubator (TVS-126MA, Advantech Toyo, Japan).

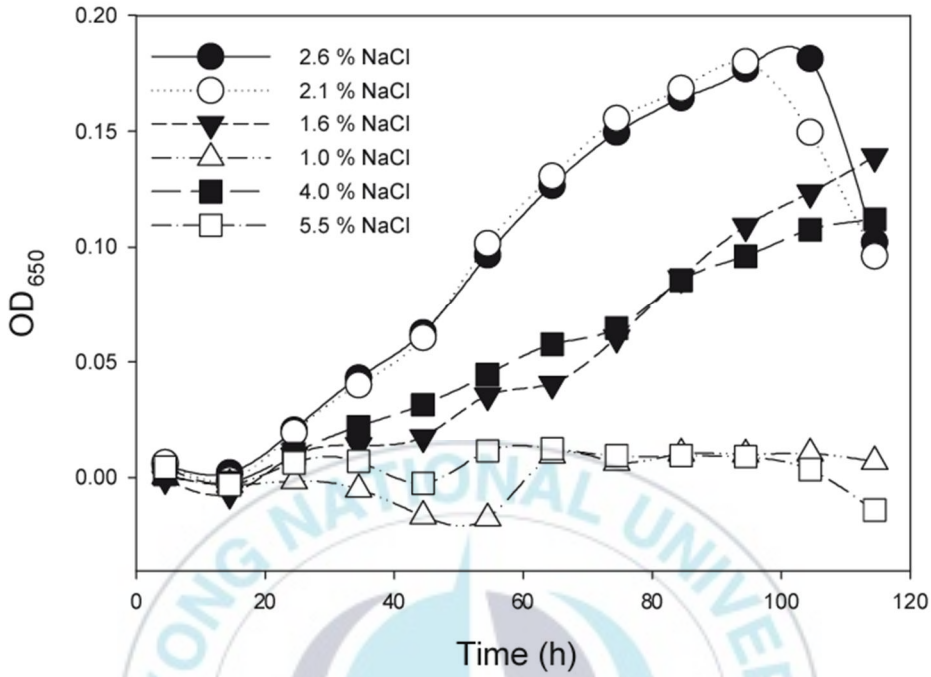

Fig. 9. Hydrogen ion concentration range for the growth of strain IMCC1322.

OD measurements at 650 nm were recorded using a temperature gradient incubator (TVS-126MA, Advantech Toyo, Japan). The cells were cultured at 25 ℃.

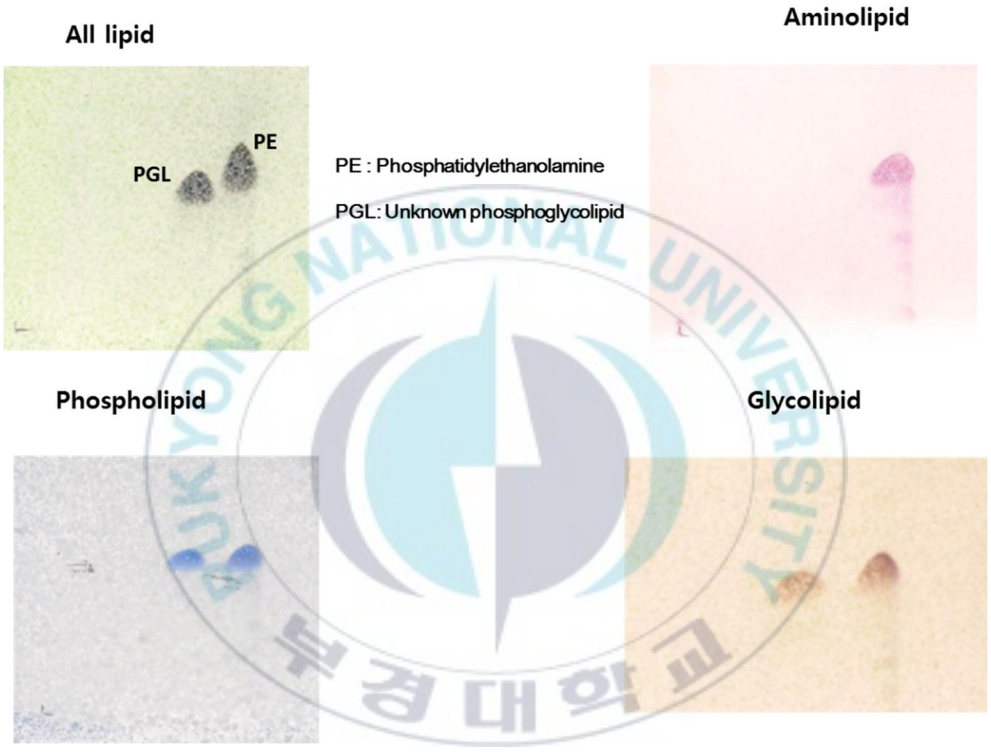

Fig. 10. Polar lipid profile of strain IMCC1322.

Phosphoethanolamine and unknown phosphoglycolipid were detected by using standard methods.

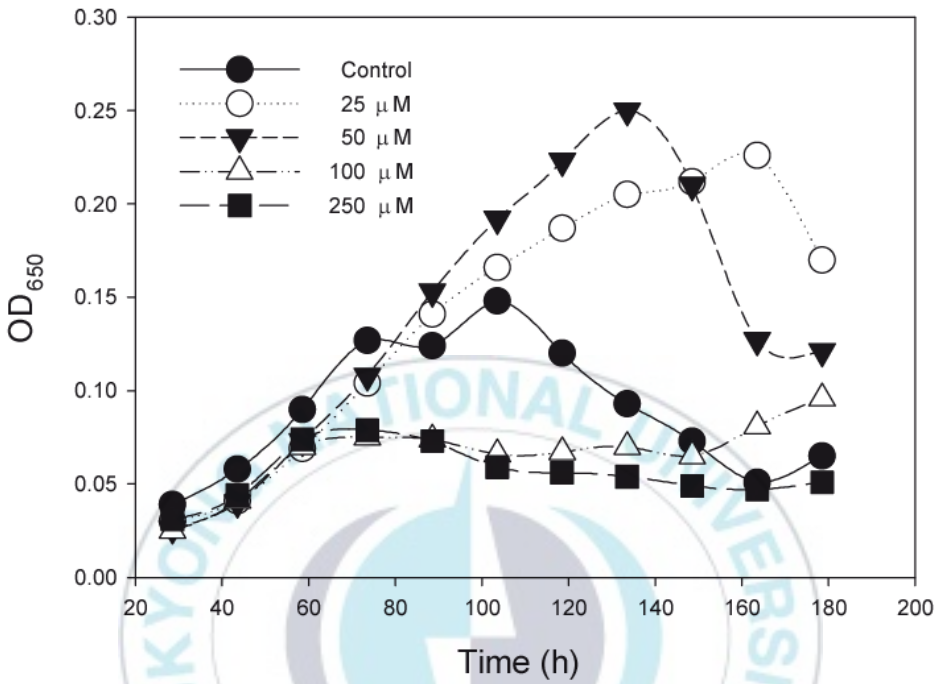

Fig. 11. Growth of IMCC1322 cultures in the presence of various DMSP concentrations.

The best growth was observed at 50 μM DMSP. OD measurements at 650 nm were recorded using a temperature gradient incubator (TVS-126MA, Advantech Toyo, Japan).

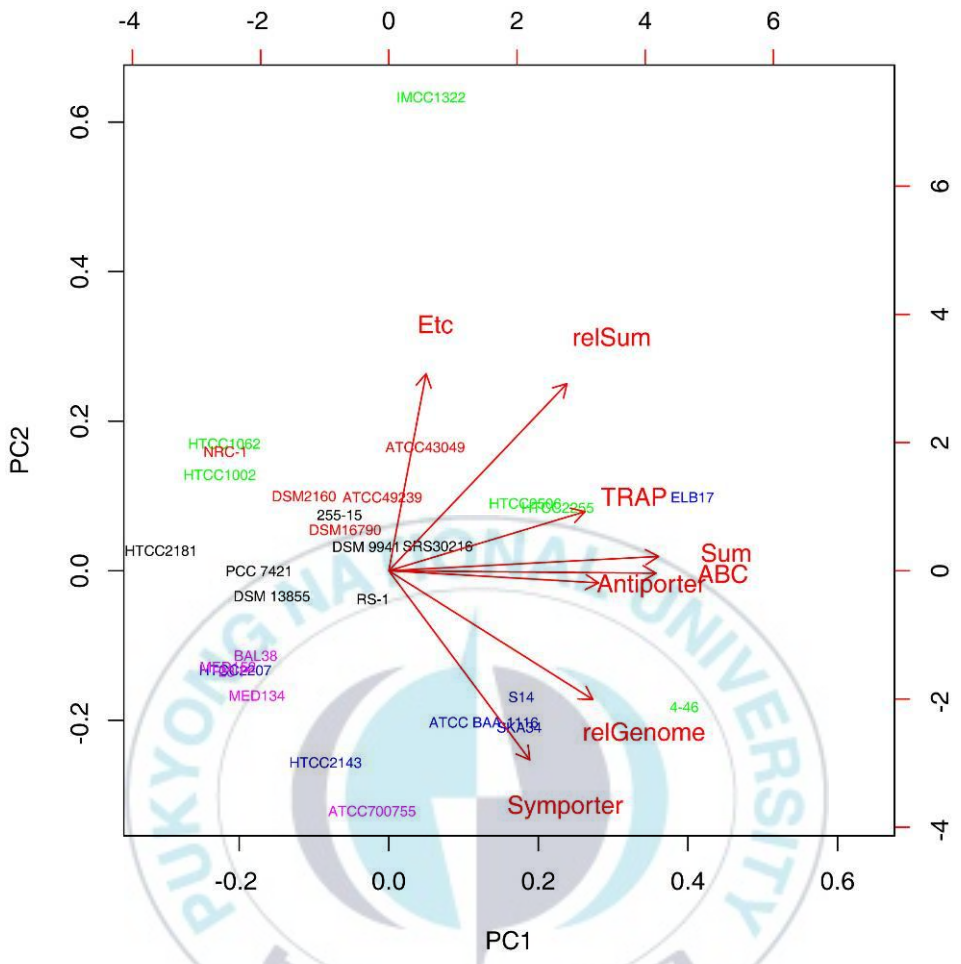

Fig. 12. Principal component analysis of the relative membrane transporter abundances in light-utilizing archaea and bacteria encoding the retinylidene protein.

The following coloring scheme is used: Halobacteria (red), Alphaproteobacteria (green), Gammaproteobacteria (blue), Flavobacteriia (magenta), and other bacteria (black). Percentile data from Table 9 were analyzed using the "prcomp" function in R package (version 2.12.0), and were plotted against the first two principal components PC1 (52.7%) and PC2 (21.3%).

적 요

IMCC1322 균주는 동해의 표층수(surface water)에서 분리되었으며, 16S rRNA 분석 결과 SAR116 의 OCS28 의 하위계통(sub-clade)에 속하는 것으로 밝혀졌다. 대수기(logarithmic-phase) 배양에서 짧은 비브리오드(vibrioids)로 나타났으며, 마이토마이신(mitomycin) 또는 장시간 배양(aged culture)에서 길쭉한 나선형으로 보였다.

IMCC1322 균주의 성장 특성(Growth characteristics)은 게놈(genomic) 정보에 기초하여 평가되었다. IMCC1322 게놈(genome)은 프로테오로돕신 (PR), 일산화탄소 탈수소 효소(carbon monoxide dehydrogenase) 및 DMSP(dimethylsulfoniopropionate) 활용 효소를 코드한다. IMCC1322 의 PR(proteorhodopsin)은 세포질 막(cytoplasmic membrane)에서 빛에 의해 구동되는 양성자 펌프(proton pump) 역할을 하는 기능성 레티닐리딘 단백질(retinylidene protein)의 특성을 가진다. 그러나, IMCC1322 균주의 잠재적인 PR 의존성 광 영양 활동(PR-dependent phototrophic potential)은 일산화탄소 및 영양소가 제한된 배양 조건에서만 관찰되었으며, DMSP, 개미산염, 및 메탄설폰산염(methane sulfonate)를 이용한 성장 반응이 관찰되었다.

IMCC1322 배양 분석 결과, 바다의 유광층에서 미생물 군집(microbial community)의 우점하는 SAR116 그룹의 특징으로 생물지구화학(biogeochemical)의 과정이 밝혀졌다. 또한, IMCC1322 균주의 다상적 분류(polyphasic taxonomy)는 화학분류(chemotaxonomic) 시험 외에 16S rRNA 계통 발생(phylogeny) 및 배양 분석에 의해 *Candidatus* Puniceispirillum marinum 을 제안 하였다.

감사의 글

미생물이라는 학문을 학부에서 접하고 졸업 후 개인적으로 많은 부족함을 느꼈습니다. 이러한 부족함을 채우기 위하여 대학원 진학을 통하여 더 많은 지식을 얻기 위해 지도교수님이신 오현명 교수님을 찾아뵙고 제가 배우고 싶은 부분과 더 나아가 교수님의 지식을 얻어 더 발전하고 싶었습니다.

항상 더 많은 가르침을 주신 오현명 교수님께 진심으로 감사 드리며, 학문 이외에 개인적으로 궁금했던 내용들과 더 많은 경험을 하게 해주신 교수님께 다시 한번 감사드립니다.

또한, 석사논문을 꼼꼼하게 검토해 주시고 개인적으로 더 발전할 수 있게 도와주신 경성대학교 조영근 교수님과 부산대학교 이준희 교수님께도 진심으로 감사의 말씀을 전해 드립니다.

회사에 다니는 와중에 발표 자료나 과제가 많을 때 도와준 정안이, 정희에게 고맙다는 말을 전하며 너희가 많이 도와준 덕분에 이렇게 좋은 결과를 얻지 않았을까 생각한다.

또한, 개인적인 학위임에도 불구하고 도와주신 김영수 본부장님과 옆에서 항상 응원해준 양준혁 선임님, 정경이누나, 수연이누나, 선연이, 형민이, 은이, 철회행님, 보람이, 희정이, 한필이, 재열이에게 진심으로 감사의 말씀 전합니다.

학위 과정에서 회사일과 동시에 하는 것이 힘들어 포기하려고 했을 때 진심으로 격려해주고 잘해보자는 마음을 가지게 해주신 이두별 센터장님께도 진심으로 감사 드립니다.

마지막으로, 은호가 막 태어나 학위 과정을 회사 생활과 동시에 할 수 있을까 고민하고 있을 때 고민 자체를 없애준 우리 소은이와 격려해주신 부모님, 그리고 우리 은호, 도겸이에게 진심으로 감사의 말을 전합니다.